الجمهورية الجزائرية الديمقراطية الشعبية
THE PEOPLE'S DEMOCRATIC REPUBLIC OF ALGERIA
وزارة التعليم العالي والبحث العلمي
THE MINISTRY OF HIGHER EDUCATION AND SCIENTIFIC RESEARCH
جامعة عمّار ثليجي بالأغواط
AMAR TELIDJI UNIVERSITY OF LAGHOUAT
كلية التكنولوجيا
FACULTY OF TECHNOLOGY
قسم الالكتروتقني
DEPARTMENT OF ELECTROTECHNIC

Master's dissertation

Domain: Science and Technology
Field: Automatic
Option: Automatic and systems

By:

Abdi Mohammed Rafik
Alili Mohamed

THEME

Analysis of Boost Converter Topologies for Photovoltaic Systems Under Partial Shading Conditions

M. Kouzi Katia	*Pr. (President)*
Mr. Bessedik Sid Ahmed	*Pr. (Examiner)*
Mr. BENMOUIZA Khalil	*Pr. (Supervisor)*
Mr. Mouhoub birane	*MCA (co-supervisor)*

Academic year 2024/2025

ملخص:

يشهد دمج الأنظمة الكهروضوئية (PV) في شبكات الطاقة والتطبيقات المستقلة توسعًا متسارعًا نتيجةً للطلب المتزايد على مصادر الطاقة المستدامة. غير أن كفاءة هذه الأنظمة تتأثر بشكل ملحوظ بتغيرات الإشعاع الشمسي، خصوصًا في ظل ظروف التظليل الجزئي .(PSC) لمواجهة الآثار السلبية لهذه الظروف وتحسين تحويل الطاقة، تم تطوير ودراسة طوبولوجيات متعددة لمحولات الرفع على نطاق واسع. يقدم هذا العمل تحليلًا شاملًا لعدد من طوبولوجيات محولات الرفع المصممة خصيصًا للأنظمة الكهروضوئية العاملة تحت تأثير التظليل الجزئي، بما في ذلك المحولات التقليدية، والمتداخلة، والتربيعية، ومحولات المكثف المتبدل. وتتناول الدراسة أداء هذه الطوبولوجيات من حيث مكسب الجهد، والكفاءة، وجودة الطاقة. كما يتم تقييم تأثير ظروف التظليل الجزئي على القدرة الناتجة وفعالية تتبع نقطة القدرة القصوى (MPPT) لكل طوبولوجيا، مما يوفّر رؤية واضحة حول مدى ملاءمتها للأنظمة الكهروضوئية في بيئات شمسية متغيرة. تؤكد النتائج على أهمية اختيار طوبولوجيا مناسبة لتعزيز كفاءة استغلال الطاقة وتقليل الخسائر الناتجة عن التظليل.

الكلمات المفتاحية: الأنظمة الكهروضوئية(PV) ، ظروف التظليل الجزئي(PSC) ، طوبولوجيات محولات الرفع، تتبع نقطة القدرة القصوى(MPPT) ، مكسب الجهد، كفاءة الطاقة.

Abstract:

The integration of photovoltaic (PV) systems into power grids and standalone applications is rapidly expanding due to the growing demand for sustainable energy sources. However, the efficiency of these systems is highly sensitive to fluctuations in solar irradiance, particularly under partial shading conditions (PSC). To address the negative impact of PSC and improve energy conversion, various boost converter topologies have been extensively studied and developed. This work provides a comprehensive analysis of different boost converter configurations designed for PV systems operating under PSC, including conventional, interleaved, quadratic, and switched-capacitor converters. Their performance is evaluated in terms of voltage gain, efficiency, and power quality. In addition, the study assesses the influence of PSC on power output and maximum power point tracking (MPPT) capabilities for each topology, offering valuable insights into their suitability for PV systems under dynamically varying solar conditions. The findings highlight the critical importance of selecting the appropriate converter topology to maximize energy harvesting and minimize power losses in shaded environments.

Keywords: Photovoltaic (PV) Systems, Partial Shading Conditions (PSC), Boost Converter Topologies, Maximum Power Point Tracking (MPPT), Voltage Gain, Power Efficiency.

Résumé :

L'intégration des systèmes photovoltaïques (PV) dans les réseaux électriques et les applications autonomes connaît une croissance rapide en raison de la demande croissante en solutions énergétiques durables. Toutefois, l'efficacité de ces systèmes est fortement influencée par les variations de l'irradiance solaire, en particulier dans des conditions d'ombrage partiel (PSC). Pour atténuer les effets négatifs du PSC et améliorer la conversion énergétique, différentes topologies de convertisseurs élévateurs de tension ont été largement étudiées et développées. Ce travail propose une analyse approfondie de plusieurs topologies de convertisseurs adaptées aux systèmes PV fonctionnant sous PSC, notamment les convertisseurs conventionnels, entrelacés, quadratiques et à condensateur commuté. Les performances de chaque configuration sont évaluées en termes de gain de tension, de rendement énergétique et de qualité de puissance. En outre, l'étude examine l'impact du PSC sur la puissance de sortie et sur la capacité de suivi du point de puissance maximale (MPPT), apportant des éléments pertinents sur leur adaptation aux conditions solaires dynamiques. Les résultats mettent en évidence l'importance cruciale du choix de la topologie de conversion pour optimiser la récupération d'énergie tout en minimisant les pertes en cas d'ombrage partiel.

Mots-clés : Systèmes photovoltaïques (PV), Conditions d'ombrage partiel (PSC), Topologies de convertisseurs élévateurs, Suivi du point de puissance maximale (MPPT), Gain de tension, Rendement énergétique.

Acknowledgements

First and foremost, we extend our deepest gratitude to **ALLAH S.W.T** for granting us the strength, guidance, and opportunity to successfully complete our master's dissertation.

We would like to sincerely thank our supervisor, **Pr. BENMOUIZA Khalil**, for his invaluable support, insightful guidance, and constructive feedback throughout our master's journey. His expertise and encouragement have played a crucial role in the completion of this research and the writing of this dissertation.

Our heartfelt thanks also go to our co-supervisor, **Pr. BIRANE Mouhoub**, for his unwavering support, continuous availability, and valuable advice, which were essential to the successful realization of this work.

We are also grateful to the members of the jury for honoring us by evaluating our work and for their valuable insights and suggestions, which will undoubtedly enrich our academic experience.

Lastly, we would like to express our appreciation to all the professors, administrative staff, and technicians of the Department of Electrical Engineering at **Amar Telidji University of Laghouat** for their constant cooperation and support throughout our studies.

Dedication

This dissertation is dedicated to my family for their unwavering support and love, and to myself for the perseverance and hard work that made this possible.

To my friends, thank you for your encouragement and companionship during difficult times.

To my partner, ***ALILI Mohammed****, your dedication and teamwork were key to our success.*

To my advisor, thank you for your valuable guidance and support throughout this journey.

Finally, to all who believe in knowledge and excellence — you are my inspiration.

– ABDI Mohammed Rafik

This dissertation is dedicated to my parents for their unwavering support, to my siblings for their encouragement, and to myself for the perseverance throughout this journey.

To my professors and mentors, thank you for your guidance.

To my partner, ***ABDI Mohammed Rafik****, your collaboration was key.*

And to all who inspired me — this achievement is also yours.

– ALILI Mohammed

Contents

List of Figures

List of Tables

Nomenclature

D	Duty cycle of the boost converter
I_{mp}	Current at maximum power point
I_{Ph}	Photo-generated current
I_{sat}	Diode saturation current
I_{sc}	Short circuit current
I_r	Solar irradiance
P	PV output power
P_{grid}	Power injected into the grid
R_p	Parallel resistance of the PV module
R_s	Series resistance of the PV module
V_{dc}	DC-link voltage
V_{mp}	Voltage at maximum power point
V_{oc}	Open circuit voltage
V_{pv}	PV array terminal voltage

General Introduction

The global energy landscape is undergoing a significant transformation, driven by growing environmental concerns, energy security issues, and the depletion of fossil fuels. Among the various renewable energy sources, photovoltaic (PV) systems have emerged as one of the most promising and scalable technologies due to their modularity, minimal environmental footprint, and declining cost of production (1). The increasing integration of PV systems into both grid-connected and standalone applications highlights the urgency of addressing inherent technical challenges, especially those related to energy conversion efficiency and system reliability.

A fundamental challenge in PV systems lies in the intermittent and non-uniform nature of solar irradiance, which significantly affects energy harvesting, particularly under partial shading conditions (PSC). Partial shading may arise due to surrounding objects such as trees, buildings, or passing clouds, leading to multiple peaks in the power-voltage curve and thereby complicating the task of Maximum Power Point Tracking (MPPT) (2). In such scenarios, the performance of the DC-DC converter topology and the effectiveness of the MPPT algorithm become critical factors in maintaining optimal energy extraction.

Boost converters, with their ability to adapt the PV output voltage to the required load or DC-link levels, play a crucial role in PV power conditioning. However, their performance varies considerably depending on the specific topology employed. Conventional single-boost configurations, while simple, may underperform under shading or mismatch conditions. Emerging topologies—such as interleaved, quadratic, and switched-capacitor boost converters—offer potential improvements in terms of voltage gain, ripple reduction, and efficiency, especially when used in modular or distributed PV architectures (3).

This dissertation aims to provide a comprehensive comparative analysis of five different PV system topologies interfaced with boost converters, focusing on their behavior under standard and partial shading conditions. By leveraging MATLAB/Simulink-based simulations, this work evaluates critical metrics such as DC voltage stability, MPPT response, and power delivery to the grid. The goal is to identify the most efficient and resilient architecture, offering practical insights for the design of future PV installations.

Chapter 1

Basic Principle of Photovoltaic Systems

1.1 Introduction

This chapter delves into the fundamental principles of photovoltaic energy conversion, the characteristics of PV systems, and the crucial role of MPPT. It will specifically examine the operating principles and mathematical modeling of the boost converter as an interface for MPPT, followed by a discussion on the integration of these algorithms with boost converters and associated control strategies. Various PV and DC-DC topologies will be reviewed, the objective is to provide a comprehensive understanding of how these technologies synergize to enhance the overall efficiency and effectiveness of solar PV energy systems.

1.2 Fundamentals of Solar Energy and Photovoltaic Conversion

1.2.1 Solar Radiation

The sun, a natural fusion reactor, continuously radiates an immense amount of energy into space. The Earth receives a fraction of this energy, approximately 175 petawatts over its cross-sectional area (4). The solar constant, defined as the solar power density incident on a surface perpendicular to the sun's rays at the Earth's mean distance from the sun (one astronomical unit, AU), is approximately 1367 W/m^2 (5). However, the actual solar irradiance reaching the Earth's surface is attenuated by the atmosphere and varies significantly with geographical location, time of day, season, and meteorological conditions (clouds, humidity, aerosols).

Solar geometry, describing the sun's position relative to an observer on Earth, is crucial for optimizing solar energy collection. Key parameters include:

- Latitude (ϕ): The geographic latitude of the location.
- Declination Angle (δ): The angular position of the sun at solar noon with respect to the plane of the equator, varying between -23.45° and +23.45°.
- Hour Angle (H): The angular displacement of the sun east or west of the local meridian due to Earth's rotation, with solar noon being 0°.

These parameters determine the solar altitude (α) and azimuth angle (A), which dictate the angle of incidence of solar radiation on a PV panel.(6)

1.2.2 The Photovoltaic Effect

The conversion of sunlight into electricity in a PV cell is governed by the photovoltaic effect. PV cells are typically semiconductor devices, most commonly made from silicon. In a silicon crystal, atoms are bonded covalently. Pure silicon is an intrinsic semiconductor with a specific bandgap energy ($E_g \approx 1.12$ eV at room temperature). For an electron to contribute to current flow, it must be excited from the valence band to the conduction band.(3) To create a PV cell, silicon is doped to form a p-n junction:

- n-type silicon: Doped with pentavalent impurities (e.g., phosphorus), creating an excess of free electrons.
- p-type silicon: Doped with trivalent impurities (e.g., boron), creating an excess of holes (electron vacancies).

When these two types are joined, electrons from the n-side diffuse to the p-side, and holes from the p-side diffuse to the n-side. This diffusion creates a region depleted of free charge carriers near the junction, known as the depletion region or space charge region. An internal electric field is established across this region, opposing further diffusion.

When photons with energy greater than or equal to the bandgap energy ($h\nu \geq E_g$, where h is Planck's constant and ν is the photon frequency) strike the PV cell, they can excite electrons from the valence band to the conduction band, creating electron-hole pairs. If these pairs are generated within or near the depletion region, the internal electric field separates them: electrons are swept to the n-side and holes to the p-side. This accumulation of charge creates a voltage potential across the cell. If an external circuit is connected, these separated charges can flow, producing an electric current.(7)

1.3 Photovoltaic Cell and Module Characteristics

1.3.1 Equivalent Circuit Model

The behavior of a practical PV cell can be represented by an equivalent circuit. A common model is the single-diode model, shown in Figure 1.(8)

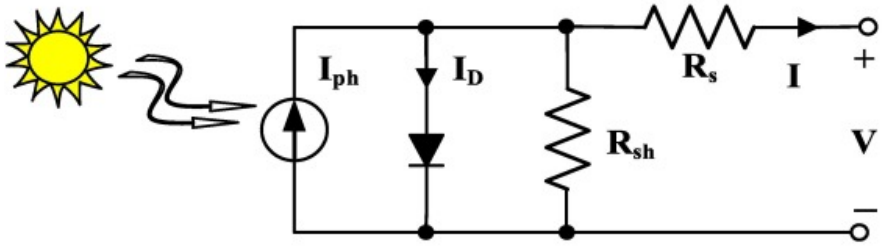

Figure 1.1: Mathematical modeling of a Single Diode PV cell

The components are:

- I_{ph}: Photocurrent, a light-generated current source directly proportional to solar irradiance.
- D: A diode representing the p-n junction.
- R_s: Series resistance, accounting for resistive losses in contacts, semiconductor material, etc.
- R_{sh}: Shunt resistance (or parallel resistance), representing leakage currents across the junction.

The current-voltage (I-V) relationship for this model is given by (8):

$$I = I_{ph} - I_d - I_{sh} \tag{1.1}$$

where I_d is the diode current and I_{sh} is the shunt current.(8)

$$I_d = I_0 \left[\exp\left(\frac{q(V + IR_s)}{nkT_c} \right) - 1 \right] \tag{1.2}$$

$$I_{sh} = \frac{V + IR_s}{R_{sh}} \tag{1.3}$$

Combining these, the I-V characteristic is (8):

$$I = I_{ph} - I_0 \left[\exp\left(\frac{q(V + IR_s)}{nkT_c} \right) - 1 \right] - \frac{V + IR_s}{R_{sh}} \tag{1.4}$$

where:

- I is the output current of the cell.
- V is the output voltage of the cell.
- I_0 is the diode reverse saturation current.
- q is the elementary charge (1.602×10^{-19} C).
- n is the diode ideality factor (typically between 1 and 2).
- k is the Boltzmann constant (1.381×10^{-23} J/K).
- T_c is the cell temperature in Kelvin.

For an ideal cell, $R_s = 0$ and $R_{sh} = \infty$, simplifying Eq. (1.4) to:

$$I = I_{ph} - I_0 \left[\exp\left(\frac{qV}{nkT_c} \right) - 1 \right] \tag{1.5}$$

1.3.2 Key Parameters from I-V and P-V Curves

The performance of a PV cell or module is characterized by its I-V and power-voltage (P-V) curves.(9)

- Short-Circuit Current (I_{sc}): The maximum current, occurring when $V = 0$. $I_{sc} \approx I_{ph}$.
- Open-Circuit Voltage (V_{oc}): The maximum voltage, occurring when $I = 0$. From Eq. (1.5) (ideal):

$$V_{oc} = \frac{nkT_c}{q} \ln\left(\frac{I_{ph}}{I_0} + 1\right) \tag{1.6}$$

- Maximum Power Point (MPP): The operating point (V_{mp}, I_{mp}) where the PV cell produces maximum power (P_{mp}).

$$P_{mp} = V_{mp} I_{mp} \tag{1.7}$$

- Fill Factor (FF): A measure of the "squareness" of the I-V curve, indicating the quality of the cell.

$$FF = \frac{V_{mp} I_{mp}}{V_{oc} I_{sc}} \tag{1.8}$$

- Efficiency (η): The ratio of maximum electrical power output to the incident solar power ($P_{in} = GA_c$, where G is irradiance in W/m^2 and A_c is cell area).

$$\eta = \frac{P_{mp}}{P_{in}} = \frac{V_{oc} I_{sc} FF}{GA_c} \tag{1.9}$$

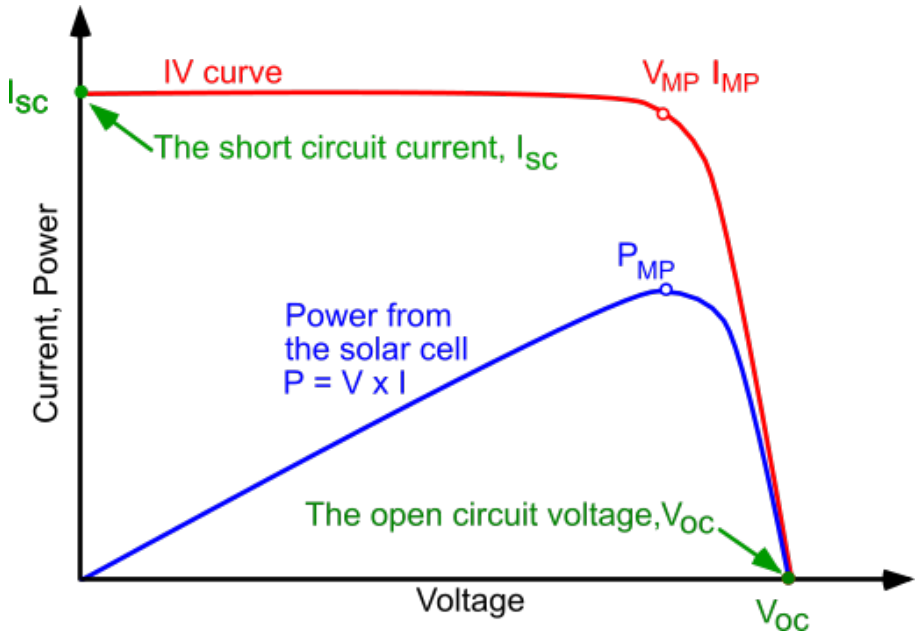

Figure 1.2: I-V and P-V curves

1.3.3 Influence of Irradiance and Temperature

- Irradiance (G): I_{sc} is directly proportional to G. V_{oc} increases logarithmically with G. Consequently, P_{mp} increases significantly with G.
- Temperature (T_c): I_{sc} increases slightly with T_c. V_{oc} decreases significantly with T_c (typically -0.2% to -0.4% per °C for silicon cells). This leads to a decrease in P_{mp} as T_c rises.

A PV module consists of multiple cells connected in series to achieve higher voltage, and strings of modules can be connected in parallel for higher current. The characteristics described apply to modules as well, with parameters scaled accordingly.(10)

1.4 The Boost Converter in PV Systems

PV modules have a unique operating point (MPP) where they deliver maximum power. This MPP varies with environmental conditions. To operate the PV module at its MPP and adapt its output voltage/current to the load or grid requirements, a DC-DC converter is essential(10). The boost converter is a step-up converter, increasing a lower DC input voltage to a higher DC output voltage. It is widely used in PV systems, especially when the PV array voltage is lower than the battery bank voltage or the DC-link voltage of a grid-tied inverter.(11)

1.4.1 Principle of Operation

A basic boost converter consists of an inductor (L), a controllable switch (S, typically a MOSFET), a diode (D), and an output capacitor (C).

Add figure of basic boost converter

The operation can be analyzed in two states, assuming Continuous Conduction Mode (CCM), where the inductor current (I_L) never falls to zero:

1. **Switch S is ON (Charging State, duration DT_s):** The input voltage V_{in} is applied across the inductor L. The inductor current I_L ramps up linearly, storing energy in its magnetic field. The diode D is reverse-biased, and the capacitor C supplies current to the load R. Voltage across inductor:
$$V_L = V_{in} \tag{1.10}$$
Rate of change of inductor current:
$$\frac{dI_L}{dt} = \frac{V_{in}}{L} \tag{1.11}$$
2. **Switch S is OFF (Discharging State, duration $(1-D)T_s$):** The switch S opens. The inductor L opposes any sudden change in current. The inductor current now flows through the diode D, charging the capacitor C and supplying the load R. The voltage across the inductor reverses polarity. Voltage across inductor:
$$V_L = V_{in} - V_{out} \tag{1.12}$$

Rate of change of inductor current:

$$\frac{dI_L}{dt} = \frac{V_{in} - V_{out}}{L} \tag{1.13}$$

Here, D is the duty cycle of the switch (fraction of time the switch is ON) and T_s is the switching period ($T_s = 1/f_s$, where f_s is the switching frequency).(2)

1.4.2 Mathematical Modeling (Steady-State)

Under steady-state conditions, the average voltage across the inductor over one switching period is zero (volt-second balance):

$$V_{in}(DT_s) + (V_{in} - V_{out})((1 - D)T_s) = 0 \tag{1.14}$$

$V_{in}D + (V_{in} - V_{out})(1 - D) = 0$
$V_{in}D + V_{in} - V_{in}D - V_{out} + V_{out}D = 0$
$V_{in} - V_{out}(1 - D) = 0$
Thus, the voltage conversion ratio is:

$$\frac{V_{out}}{V_{in}} = \frac{1}{1 - D} \tag{1.15}$$

Since $0 < D < 1$, V_{out} is always greater than or equal to V_{in}.

The average current through the capacitor over one switching period is zero (charge balance). Assuming lossless operation, input power $P_{in} = V_{in}I_{in}$ equals output power $P_{out} = V_{out}I_{out}$.
$V_{in}I_{in} = V_{out}I_{out}$

$$\frac{I_{out}}{I_{in}} = \frac{V_{in}}{V_{out}} = 1 - D \tag{1.16}$$

So, the boost converter steps up voltage while stepping down current.

Inductor Current Ripple (ΔI_L): During the ON state:

$$\Delta I_L = \frac{V_{in}}{L} DT_s \tag{1.17}$$

Output Voltage Ripple (ΔV_{out}): During the ON state (when capacitor supplies load):

$$\Delta V_{out} \approx \frac{I_{out}DT_s}{C} = \frac{V_{out}}{R}\frac{DT_s}{C} \tag{1.18}$$

(Approximation, more accurate form considers capacitor discharge waveform).(12)

1.4.3 Efficiency Considerations

The efficiency of a boost converter (η_{conv}) is affected by:

- Conduction Losses: Due to MOSFET $R_{ds(on)}$, diode forward voltage (V_F), inductor DC resistance (DCR), and capacitor Equivalent Series Resistance (ESR).

- Switching Losses: Occur in the MOSFET during turn-on and turn-off transitions (due to simultaneous non-zero voltage and current) and diode reverse recovery.

$$\eta_{conv} = \frac{P_{out}}{P_{in\_actual}} = \frac{P_{out}}{P_{out} + P_{losses}} \tag{1.19}$$

High efficiency (e.g., >90-98%) is crucial in PV systems to avoid wasting the harvested solar energy.(12)

1.5 Maximum Power Point Tracking (MPPT)

1.5.1 Importance of MPPT

As shown in Figure (1.2), a PV module has a single operating point (MPP) on its P-V curve where power output is maximized. This MPP is not fixed; it shifts with changes in solar irradiance and cell temperature. Directly connecting a PV module to a load results in an operating point determined by the intersection of the PV module's I-V curve and the load's characteristic. This point is rarely the MPP.(13)

MPPT is an electronic control technique that continuously adjusts the apparent load seen by the PV module to force its operation at or very near the MPP, thereby maximizing the extracted power under all conditions.(14)

1.5.2 Overview of MPPT Algorithms

Numerous MPPT algorithms have been developed, varying in complexity, tracking speed, accuracy, cost, and implementation ease. The output of an MPPT algorithm is typically a control signal (e.g., duty cycle D for a DC-DC converter) that adjusts the PV module's operating point.

Perturb and Observe (P&O) Algorithm

P&O is one of the most common MPPT algorithms (Figure (1.3)) due to its simplicity.(15)

- **Principle:** The algorithm periodically perturbs (i.e., slightly increases or decreases) the PV module's operating voltage (or current) and observes the resulting change in output power.
  - If $dP/dV > 0$ (power increases with voltage increase), the perturbation was in the correct direction, and the next perturbation continues in that direction.
  - If $dP/dV < 0$ (power decreases with voltage increase), the perturbation was in the wrong direction, and the next perturbation reverses direction.
- **At MPP:** The condition is $dP/dV = 0$.
- **Implementation:**
  1. Measure current $I(k)$ and voltage $V(k)$.
  2. Calculate power $P(k) = V(k)I(k)$.

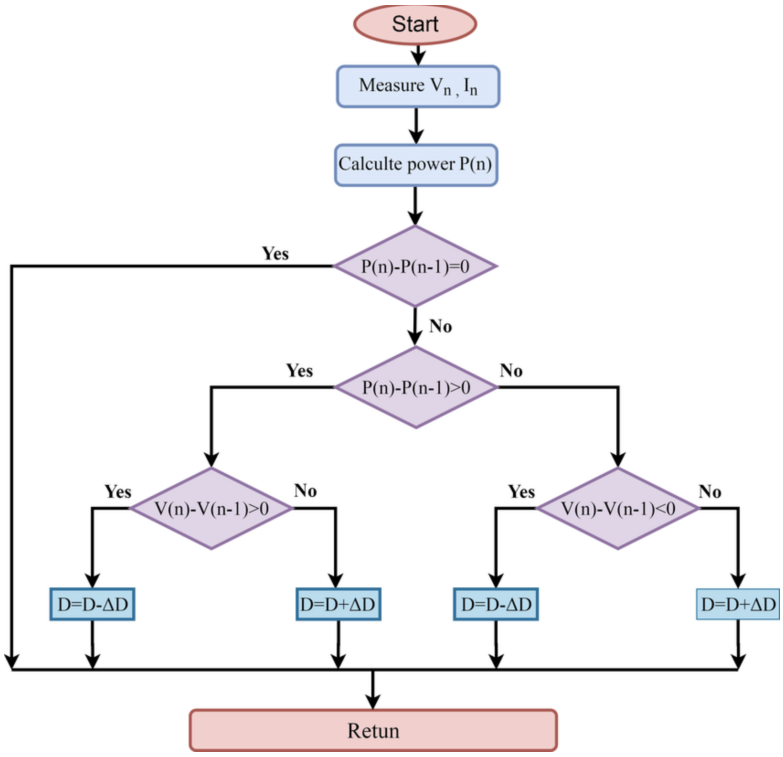

Figure 1.3: Perturb and observe MPPT flowchart

3. Compare $P(k)$ with previous power $P(k-1)$ and $V(k)$ with $V(k-1)$.
4. If $P(k) > P(k-1)$: If $V(k) > V(k-1)$, increase voltage (e.g., decrease duty cycle D for a boost converter connected to PV output). Else ($V(k) < V(k-1)$), decrease voltage (e.g., increase D).
5. If $P(k) < P(k-1)$: If $V(k) > V(k-1)$, decrease voltage. Else ($V(k) < V(k-1)$), increase voltage.

- **Advantages:** Simple, low computational cost.
- **Disadvantages:** Oscillations around the MPP in steady-state, potential for tracking in the wrong direction during rapidly changing irradiance (16).

1.6 Integration of MPPT with Boost Converters

When a boost converter is used in a PV system, the PV module is connected to the input of the converter ($V_{in} = V_{pv}$, $I_{in} = I_{pv}$). The MPPT algorithm controls the duty cycle D of the boost converter's switch .

By varying D, the effective input impedance seen by the PV module is changed: $R_{in\_eff} = V_{pv}/I_{pv}$ From Eq. (1.15), $V_{pv} = V_{in} = V_{out}(1-D)$. Assuming the output V_{out} is relatively stable (e.g., connected to a battery or stable DC link), changing D directly influences V_{pv}. The MPPT algorithm adjusts D to move V_{pv} (and consequently I_{pv}) along the PV module's I-V curve until the operating point coincides with the MPP.

For example, using P&O with a boost converter:

- If the algorithm decides to increase V_{pv} (move towards V_{oc}), it must decrease D.
- If the algorithm decides to decrease V_{pv} (move towards I_{sc}), it must increase D.

This control forms a closed-loop system where the PV voltage and current are sensed, the MPPT algorithm processes this information, and the duty cycle of the PWM signal driving the boost converter switch is adjusted accordingly. The sampling rate of PV parameters and the perturbation step size for D are critical design parameters affecting tracking speed and steady-state oscillation.(15)

1.7 Control Strategies for Boost Converters in MPPT Applications

The MPPT algorithm determines the desired operating point (e.g., target V_{pv} or target D). The control system for the boost converter then implements this. Typically, a Pulse Width Modulator (PWM) generates the gate signal for the MOSFET switch (S). The MPPT algorithm provides the reference for this PWM, which is often the duty cycle D.

1.7.1 Direct Duty Cycle Control

The MPPT algorithm directly computes the change in duty cycle (ΔD) or the absolute duty cycle D needed to track the MPP. This D is then fed to the PWM generator. This is common with P&O and INC algorithms.(13)

1.7.2 Voltage/Current Control Loops

More sophisticated control might involve inner control loops. For instance:

1. The MPPT algorithm determines a reference voltage V_{pv_ref} (which is V_{mp}).
2. A voltage controller (e.g., a Proportional-Integral, PI, controller) compares the actual V_{pv} with V_{pv_ref}.
3. The output of this voltage controller determines the duty cycle D for the PWM generator.

$$Error_V = V_{pv\_ref} - V_{pv} \tag{1.20}$$

$$D = K_{p\_v} Error_V + K_{i\_v} \int Error_V dt \tag{1.21}$$

(where K_{p_v} and K_{i_v} are PI gains for the voltage loop)

This structure can provide better regulation and disturbance rejection. The design of these control loops, including tuning of PI parameters, is crucial for stability and dynamic response. The text mentions a "Quasi-Double-Boost DC/DC Converter" [1] designed for solar PV systems, suggesting advanced converter topologies are also being explored to enhance performance, potentially offering higher voltage gain or efficiency with specialized control schemes. Such specialized converters might require tailored MPPT integration strategies.(14)

1.8 PV Array and DC/DC Converter Topologies

A primary objective of this research is to identify power electronic interface topologies that optimize maximum power extraction from photovoltaic (PV) arrays while concurrently minimizing overall system cost. To this end, a comparative study of five distinct configurations detailing the interconnection between PV arrays and DC/DC boost converters has been undertaken (11)(9). These configurations, henceforth referred to as Topologies 1 through 5, are described as follows:

1.8.1 Topology 1: Single PV + Single Boost Converter

In this fundamental configuration (Figure 1.4), a single PV unit (which could be a single module or a small, pre-configured string of modules) is directly connected to a dedicated DC/DC boost converter. The output of this boost converter is then conditioned for connection to the electricity grid or a DC load.

Rationale and Implications: This topology represents the most basic form of module-level or string-level MPPT.

- **Potential Advantages:** Simplicity in design and control. The MPPT algorithm operates optimally for the single connected PV unit, maximizing its individual power extraction without influence from other units. This can be cost-effective for very small systems or when individual panel-level optimization is paramount.
- **Potential Disadvantages:** Scalability for larger systems requires replication of many such units, which can increase overall component count and complexity compared to centralized approaches. The power processed by each converter is limited to the output of a single PV unit.

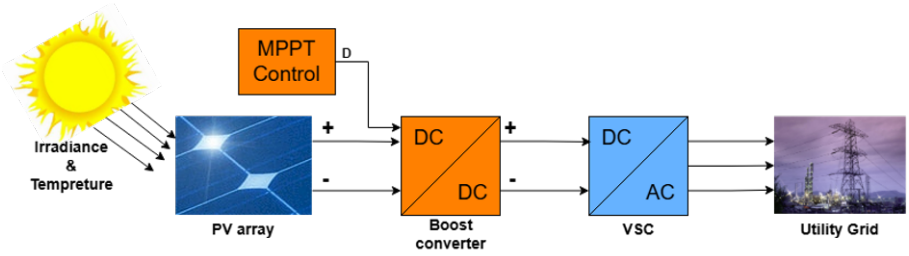

Figure 1.4: Topology 1(Single PV + Single Boost Converter)

1.8.2 Topology 2: Two Series PVs + Single Boost Converter

This configuration (Figure 1.5) involves two PV units connected in series to form a higher-voltage string. This combined string then feeds into a single, shared DC/DC boost converter. The output of this centralized boost converter is subsequently conditioned to interface with the electricity grid.

Rationale and Implications: This topology represents a common centralized MPPT approach for a small series string.

- **Potential Advantages:** The use of a single converter for two PV units can potentially reduce the per-watt cost of power electronics compared to individual converters. Series connection naturally sums voltages, which can be beneficial for achieving the necessary DC link voltage for grid interconnections with a moderate boost ratio from the converter.
- **Potential Disadvantages:** The primary drawback is its susceptibility to power losses due to mismatch between the two series-connected PV units. If the PVs experience differential shading, soiling, temperature variations, or have different electrical characteristics, the single MPPT algorithm will struggle to find a global maximum power point for the entire string. The performance will be dictated by the PV unit imposing the greatest current limitation, leading to suboptimal power harvesting from the better-performing unit.

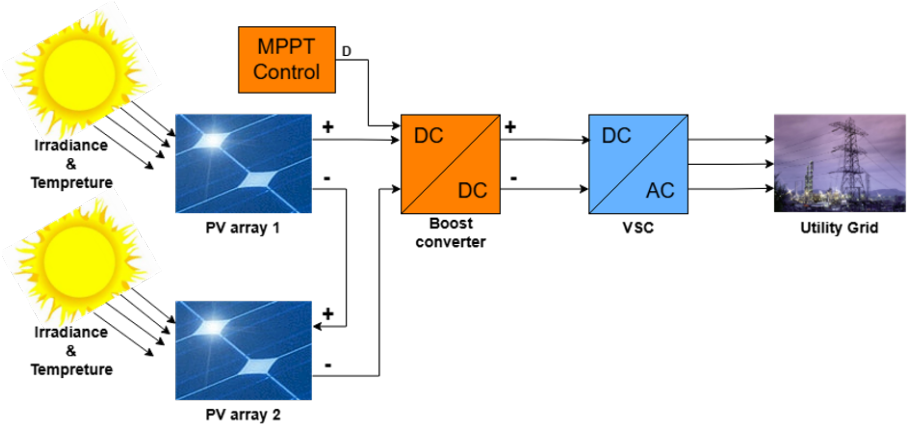

Figure 1.5: Topology 2 (Two Series PVs + Single Boost Converter)

1.8.3 Topology 3: Two Parallel PVs + Single Boost Converter

In Topology 3 (Figure 1.6), two PV units are connected in parallel. This parallel combination results in an increased current capacity at a voltage level determined by the individual PV units. This combined output then feeds into a single DC/DC boost converter, the output of which is supplied to the electricity grid.

Rationale and Implications: This is another form of centralized MPPT, but with PV units paralleled at the input.

- **Potential Advantages:** Similar to Topology 2, it utilizes a single converter, potentially offering cost benefits. If PV units are well-matched and uniformly irradiated, this can be an effective configuration. Paralleling maintains a lower input voltage to the converter compared to series connection for the same number of PV units, which might be preferable for certain boost converter designs or if high step-up ratios are to be avoided. Blocking diodes may be required for each PV unit to prevent reverse current flow.
- **Potential Disadvantages:** This topology is also susceptible to mismatch losses. If one PV unit's voltage (due to temperature, degradation, or shading) is significantly different from the other, or if its MPP voltage differs, the parallel connection can lead to circulating currents (if blocking diodes are not perfectly effective or absent) or one unit dominating and pulling the operating point away from the other's MPP. The single MPPT operates on the combined I-V characteristic. Furthermore, the input current to the boost converter will be the sum of the currents from the two PV units, requiring the converter to handle higher input currents compared to Topology 2 for the same power level.

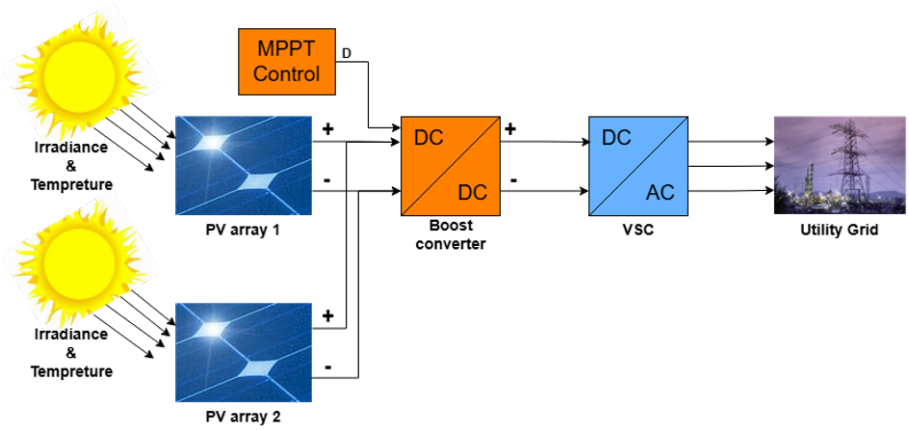

Figure 1.6: Topology 3(Two Parallel PVs + Single Boost Converter)

1.8.4 Topology 4: Two PVs with Separate Boost Converters (Series Output)

This configuration (Figure 1.7) features two PV units, each individually connected to its own dedicated DC/DC boost converter. The outputs of these two independent PV-plus-converter units are then connected in series. This series-combined DC output then feeds into the subsequent stage, such as a grid-tied inverter.

Rationale and Implications: This topology allows for independent MPPT for each PV unit while summing their output voltages.

- **Potential Advantages:** Each boost converter can independently track the MPP of its connected PV unit, significantly mitigating power losses due to inter-unit mismatches. The series connection of converter outputs results in a higher overall DC voltage, which can be advantageous for reducing current and associated resistive losses in subsequent wiring or for interfacing with high-voltage DC buses or inverters.

- **Potential Disadvantages:** This approach requires two converters, increasing initial component cost and system complexity compared to single-converter topologies. A critical challenge is ensuring proper operation with series-connected outputs; if one PV unit or its converter significantly underperforms or fails (e.g., producing very low voltage or current), it can limit the current through the entire series string of converters, thereby impacting the power delivery of the healthy unit. Coordinated control might be necessary to manage current flow and voltage balancing across the series-connected outputs.

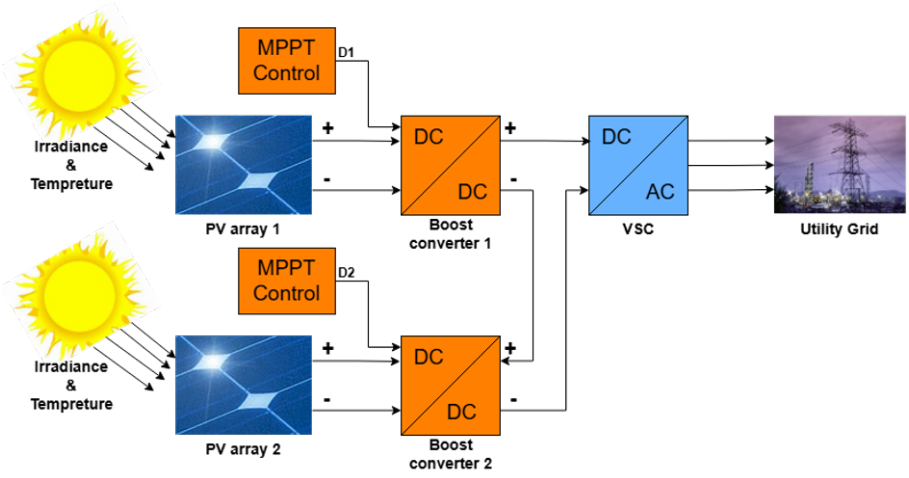

Figure 1.7: Topology 4 (Two PVs with Separate Boost Converters (Series Output))

1.8.5 Topology 5: Two PVs with Separate Boost Converters (Parallel Output)

This configuration (Figure 1.8) also involves two PV units, each individually connected to its own dedicated DC/DC boost converter. Unlike Topology 4, the outputs of these two independent PV-plus-converter units are then connected in parallel to feed the electricity grid or a common DC bus.

Rationale and Implications: This topology offers a high degree of MPPT granularity and flexibility, treating each PV unit as an independent power source whose conditioned output is combined.

- **Potential Advantages:** Maximizes energy harvest under all conditions, including severe inter-unit mismatch, as each PV unit's MPP is tracked independently by its dedicated converter. This offers the highest resilience and overall system efficiency, particularly in installations prone to partial shading or non-uniform conditions. If one unit or converter fails, the other can continue to operate and supply power.

- **Potential Disadvantages:** This topology incurs a higher cost in terms of the number of converters (one per PV unit) and increased complexity in wiring and components. Careful consideration of paralleling the converter outputs is required, potentially needing mechanisms for current sharing, synchronization, or droop control to ensure stable operation

and prevent circulating currents between converters, especially if their output voltages are not perfectly matched.

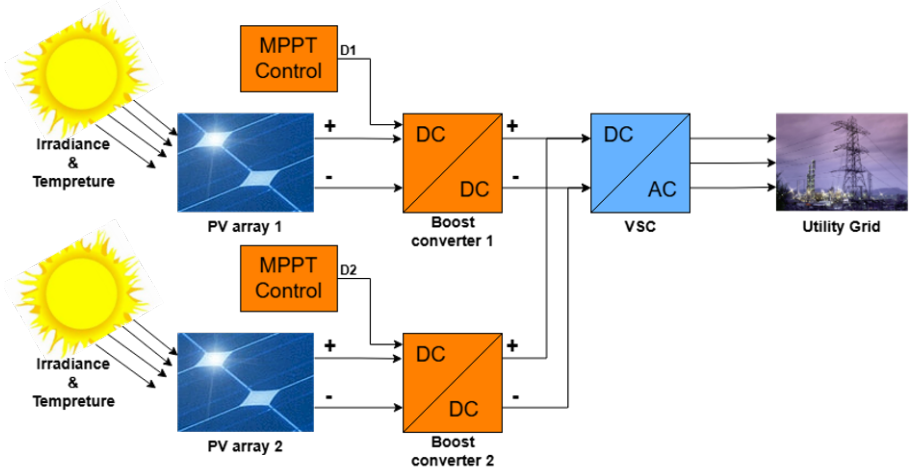

Figure 1.8: Topology 5 (Two PVs with Separate Boost Converters (Parallel Output))

The subsequent sections of this study will present the experimental and simulation results obtained from testing these four distinct topologies, with a focus on evaluating their efficacy in maximizing power extraction and their implications for system cost-effectiveness.

1.9 Conclusion

Photovoltaic systems are a cornerstone of the transition to renewable energy. Maximizing their energy yield is paramount for economic viability and resource efficiency. This chapter has outlined the fundamental principles of PV energy conversion, highlighting the non-linear characteristics of PV modules and their dependence on environmental factors.

The critical role of Maximum Power Point Tracking in dynamically adjusting the PV module's operating point to extract maximum available power has been emphasized. Common MPPT algorithms, including Perturb and Observe, Incremental Conductance, and Constant Voltage Method, were discussed, each with distinct advantages and trade-offs in terms of complexity, accuracy, and tracking speed.

The boost DC-DC converter is a key enabling technology for MPPT, providing the necessary interface to step up PV voltage and control the operating point via its duty cycle. The mathematical modeling of the boost converter elucidates its voltage and current transformation characteristics. The integration of MPPT algorithms with boost converter control, typically through PWM, forms a feedback system essential for optimal PV system performance.

Effective design and control of the MPPT-converter system, potentially using advanced converter topologies and sophisticated control strategies, are vital for improving overall PV system efficiency and reliability, thereby contributing to the wider adoption of solar energy. Further research often focuses on refining MPPT algorithms for faster and more accurate tracking under challenging conditions (e.g., partial shading, rapid irradiance changes) and developing more efficient and cost-effective power electronic converters.

Chapter 2

Simulation results and discussion

2.1 Introduction

This chapter presents the simulation-based evaluation of the five proposed PV system topologies interfaced with boost converters. The objective is to assess and compare their performance under two different solar irradiance scenarios: standard conditions and partial shading. The analysis focuses on key electrical parameters including DC-link voltage (V_{dc}), PV voltage (V_{pv}), AC grid voltage (V_{ac}), and power injected into the grid (P_{grid}). MATLAB/Simulink was used to model and simulate each topology, incorporating an MPPT control algorithm (Perturb and Observe) and voltage source conversion stage.

The simulations aim to highlight the dynamic behavior, efficiency, and robustness of each configuration, especially in the presence of environmental disturbances such as shading. Each topology is presented separately with its corresponding results, followed by a comparative discussion that summarizes the findings.

2.2 Simulink Model

The following is the Simulink model that represents the full system.

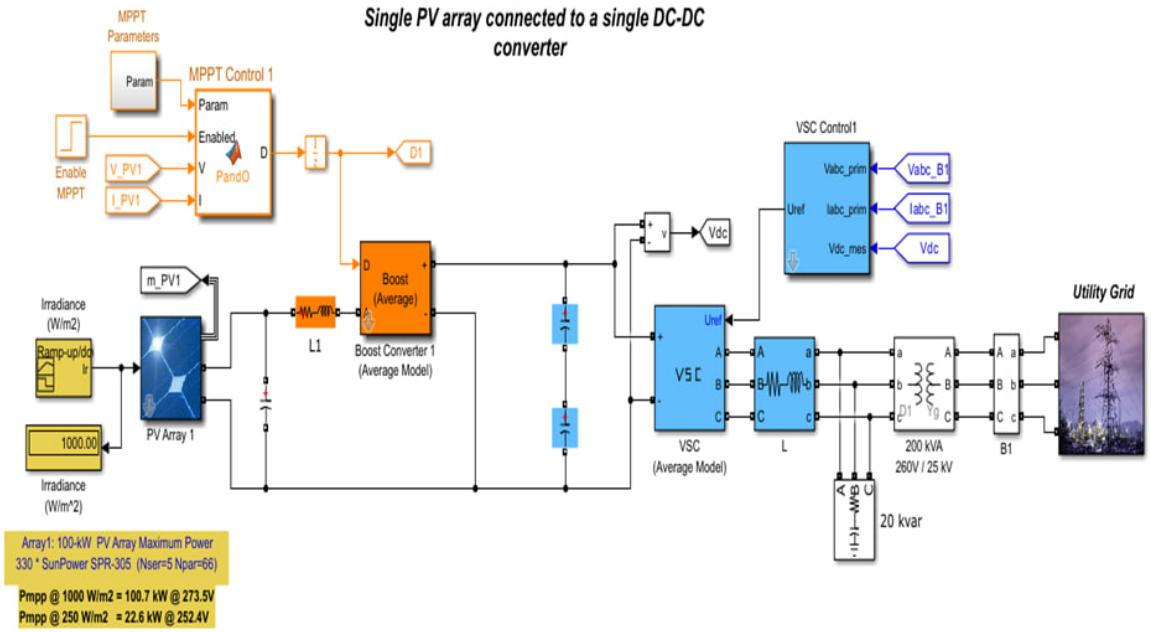

Figure 2.1: Simple Simulink model of a grid-connected PV system (topology 1)

2.2.1 PV array block

PV array consists of N_{par} strings of modules connected in parallel, each string consisting of N_{ser} modules connected in series. The *SPR-305E-WHT-D* PV module is utilized for simulation. The specifications of the module considered are tabulated in Table 2.1 under standard testing conditions (STC) of 25 °C and 1 kW/m^2.

Table 2.1: The characteristics of the PV module

Parameter	**Value**
Maximum power (P_{max})	305.226 W
Voltage at maximum power point (V_{mp})	54.7 V
Current at maximum power point (I_{mp})	5.58 A
Short circuit current (I_{sc})	5.96 A
Open circuit voltage (V_{oc})	64.2 V
Number of cells per module	96
Number of series-connected modules per string	5
Number of parallel strings	66
Series resistance (R_{s})	0.037998 Ω
Parallel resistance (R_{p})	993.51 Ω
Diode saturation current (I_{sat})	1.1753×10^{-8} A
Photo-generated current (I_{Ph})	5.9602 A
Diode quality factor (n)	1.3

I-V and P-V characteristics of the PV module considered in various irradiance situations are also shown in Fig.10

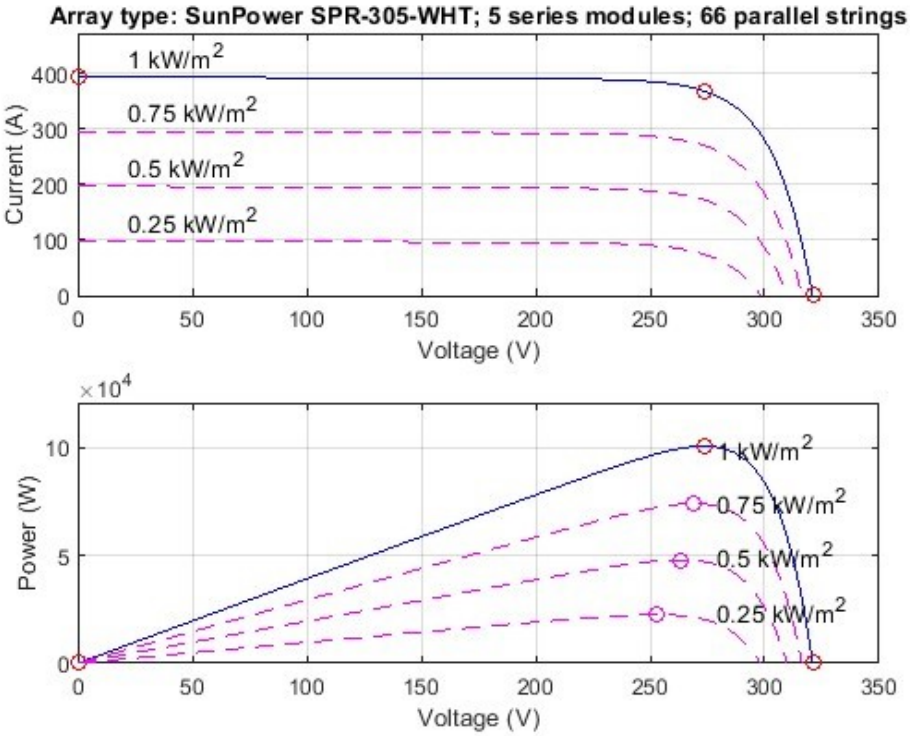

Figure 2.2: The P-V and I-V photovoltaic module's characteristics were measured at 25 °C and different levels of irradiance.

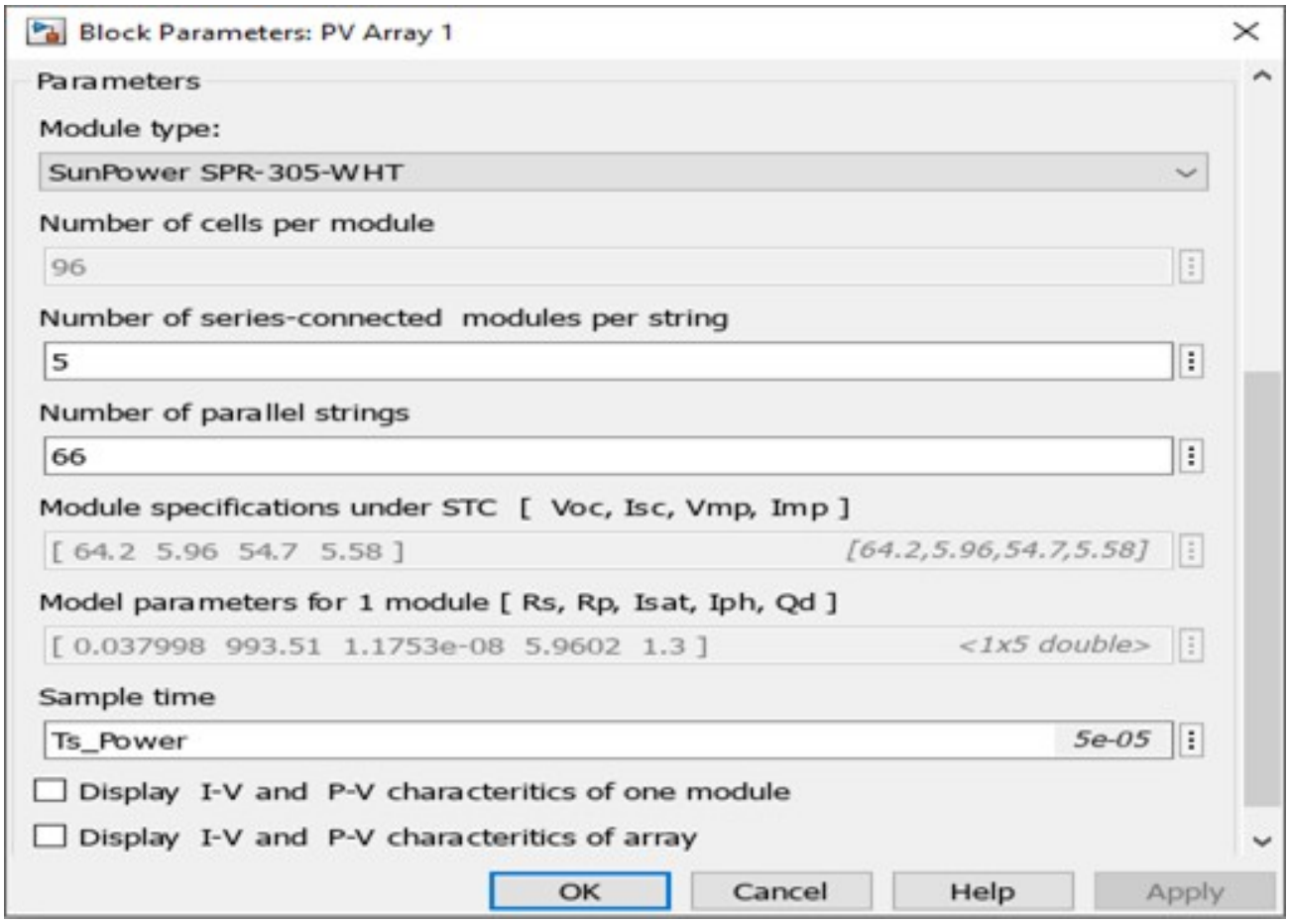

Figure 2.3: PV array block parameters in MATLAB Simulink

2.2.2 MPPT Controller (P&O Algorithm)

To ensure that the photovoltaic system operates at its maximum power point, a Perturb and Observe (P&O) MPPT algorithm was implemented in MATLAB. Adjusts the duty cycle of the boost converter based on changes in voltage and power. If power increases, the algorithm continues in the same direction; if it decreases, it reverses. Limits are set to keep the duty cycle within a safe range. The function uses persistent variables to track past values for comparison. The following code shows this implementation.

```
function D  = PandO(Param, Enabled, V, I)
% MPPT controller based on the Perturb & Observe algorithm.
% D output = Duty cycle of the boost converter (value between 0 and 1)
% Enabled input = 1 to enable the MPPT controller
% V input = PV array terminal voltage (V)
% I input = PV array current (A)
% Param input:
Dinit = Param(1);  % Initial value for D output
Dmax = Param(2);   % Maximum value for D
Dmin = Param(3);   % Minimum value for D
deltaD = Param(4); % Increment value used to increase/decrease the
   duty cycle D
% ( increasing D = decreasing Vref )
persistent Vold Pold Dold;
dataType = 'double';
if isempty(Vold)
    Vold=0;
    Pold=0;
    Dold=Dinit;
end
P= V*I;
dV= V - Vold;
dP= P - Pold;

if dP ~= 0 && Enabled ~= 0
    if dP < 0
        if dV < 0
            D = Dold - deltaD;
        else
            D = Dold + deltaD;
        end
    else
        if dV < 0
            D = Dold + deltaD;
        else
            D = Dold - deltaD;
        end
    end
else
    D = Dold;
end
if D >= Dmax || D <= Dmin
    D = Dold;
end
Dold = D;Vold = V;Pold = P;
```

Listing 2.1: Perturb and Observe MPPT Algorithm in MATLAB

2.2.3 Boost Converter

In the detailed model, the boost converter (orange blocks) in Fig. 2.4 increases the DC voltage to 500v. This converter uses an MPPT system that automatically varies the duty cycle in order to generate the required voltage to extract maximum power.

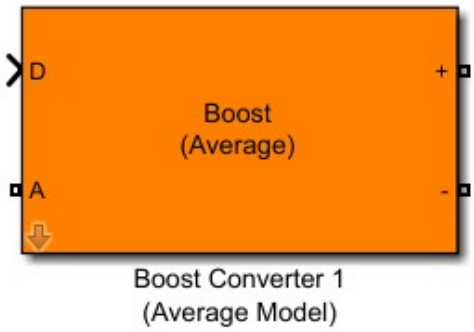

Figure 2.4: Boost Converter (Average model) block in the Simulink model

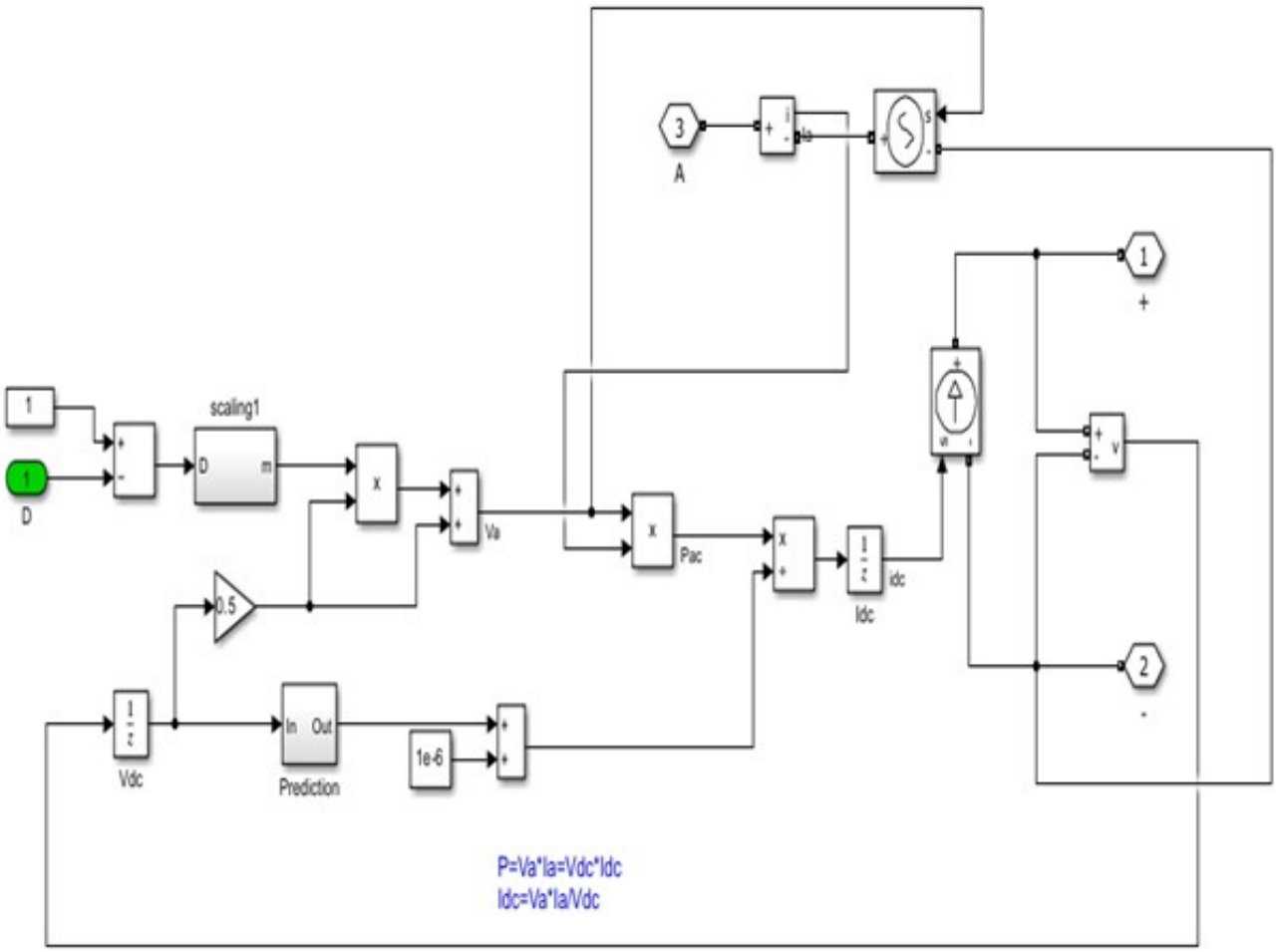

Figure 2.5: Under the mask of the "Boost Converter Control" block

2.2.4 Voltage Source Converter (VSC)

The three-level VSC (blue blocks) in Fig. 2.6 regulates the DC bus voltage at 500 V and maintains the unity power factor.(17)(18)

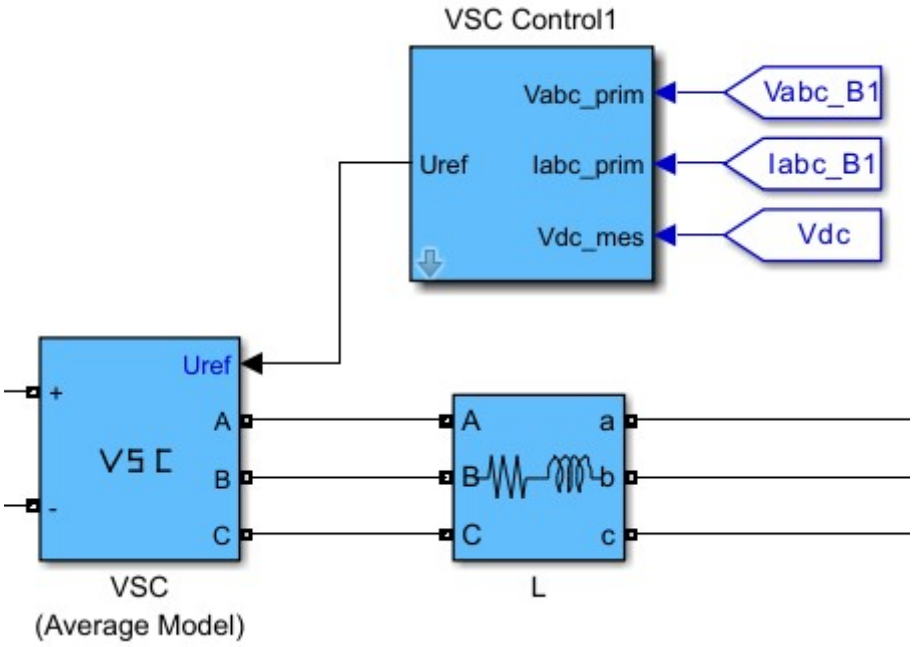

Figure 2.6: The three-level VSC

2.3 Simulation Results

The results are analyzed under two conditions: standard irradiance (1000 W/m^2) (Fig. 2.7) and partial shading (Fig. 2.8), to evaluate system stability and MPPT response.

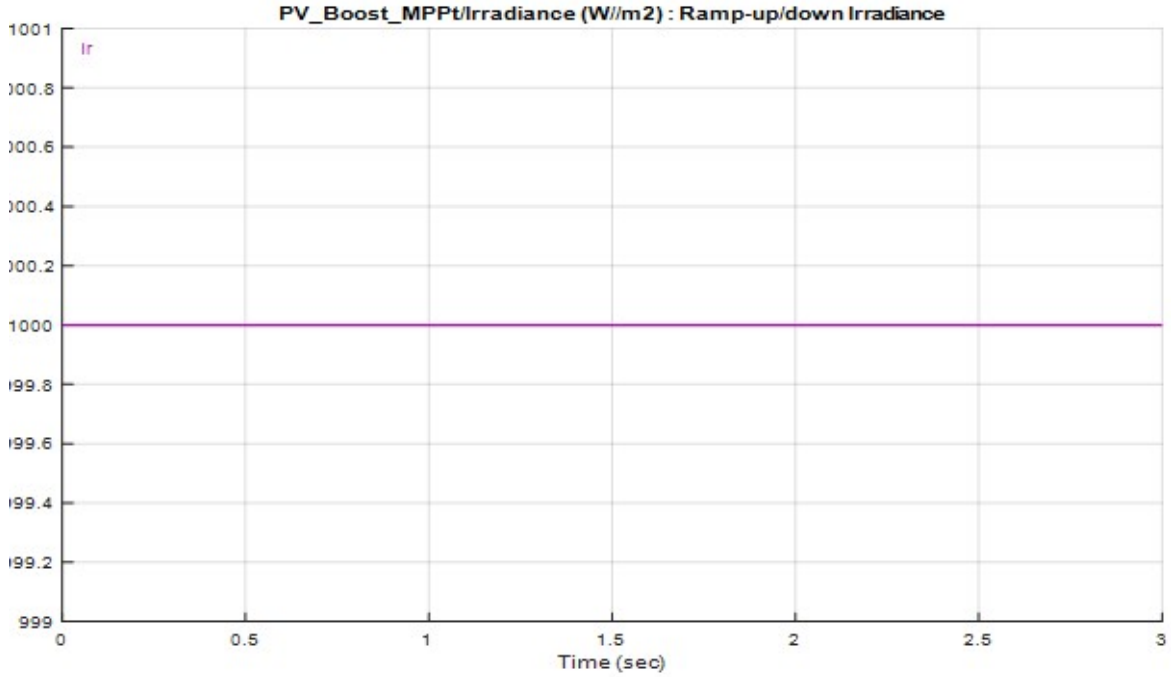

Figure 2.7: standard irradiance (1000 W/m^2)

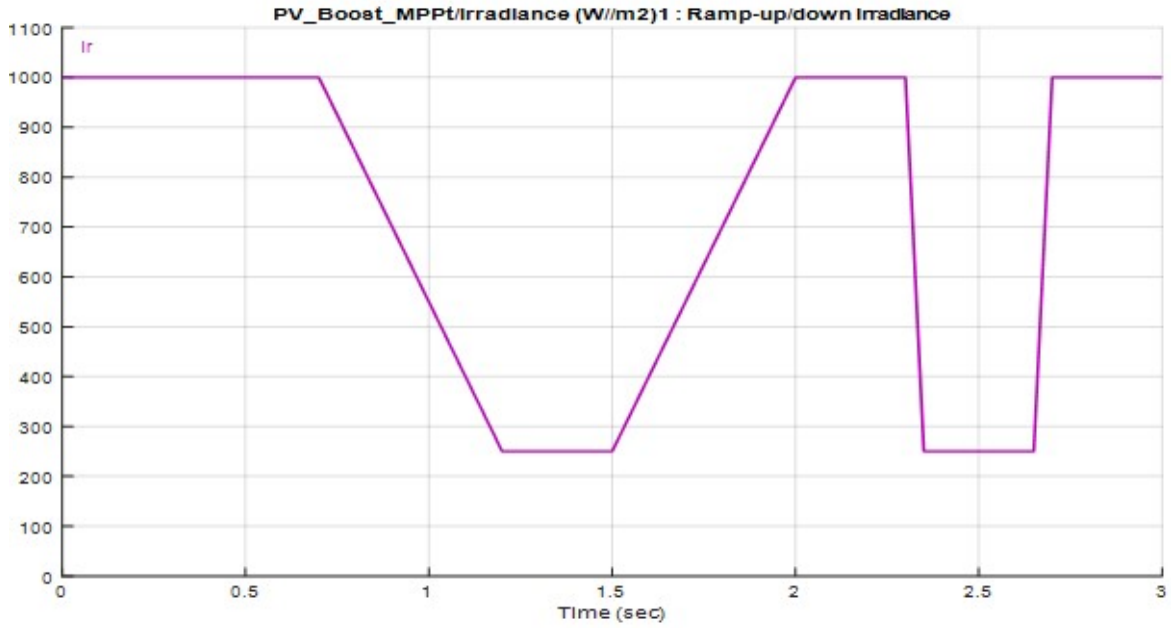

Figure 2.8: Variation of irradiance during partial shading

We present the main simulation results of each topology. Key signals such as V_{pv} (PV voltage), V_{dc} (DC link voltage), V_{ac} (AC output voltage), and P_{k} (power injected into the grid) are shown to compare system performance and energy transfer to the grid.

2.3.1 Topology 1: Single PV + Single Boost Converter

This is the most basic and straightforward topology. It consists of a single photovoltaic (PV) panel connected to a single boost converter. The main advantages are simplicity, low cost, and ease of control.

Under standard irradiance (1000 W/m^2**):**

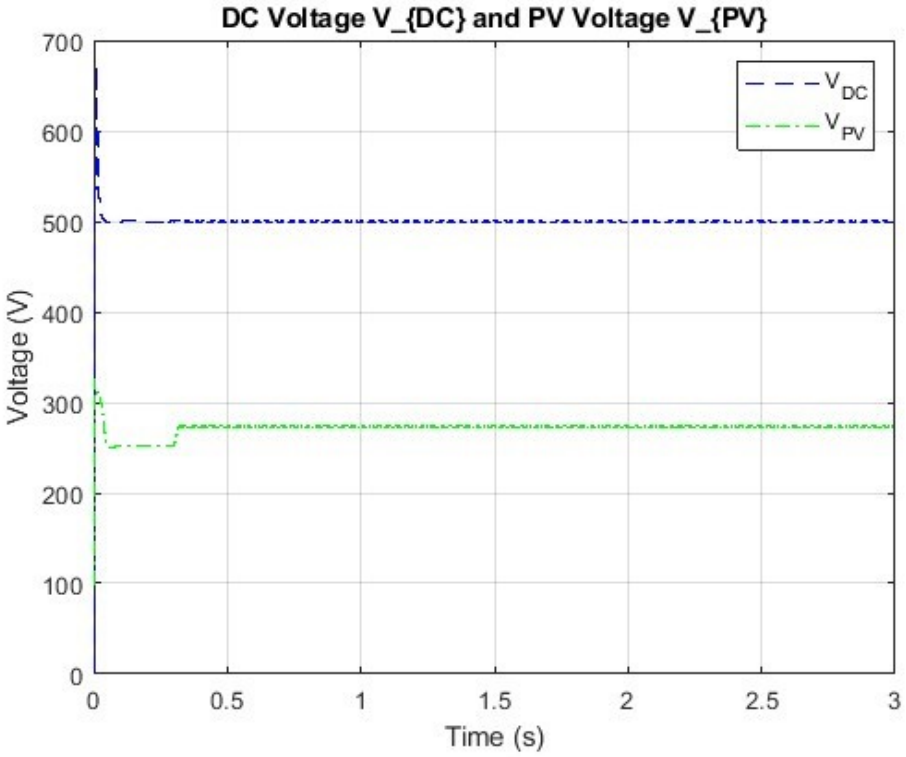

Figure 2.9: Vdc and Vpv under Standard Irradiation – Topology 1

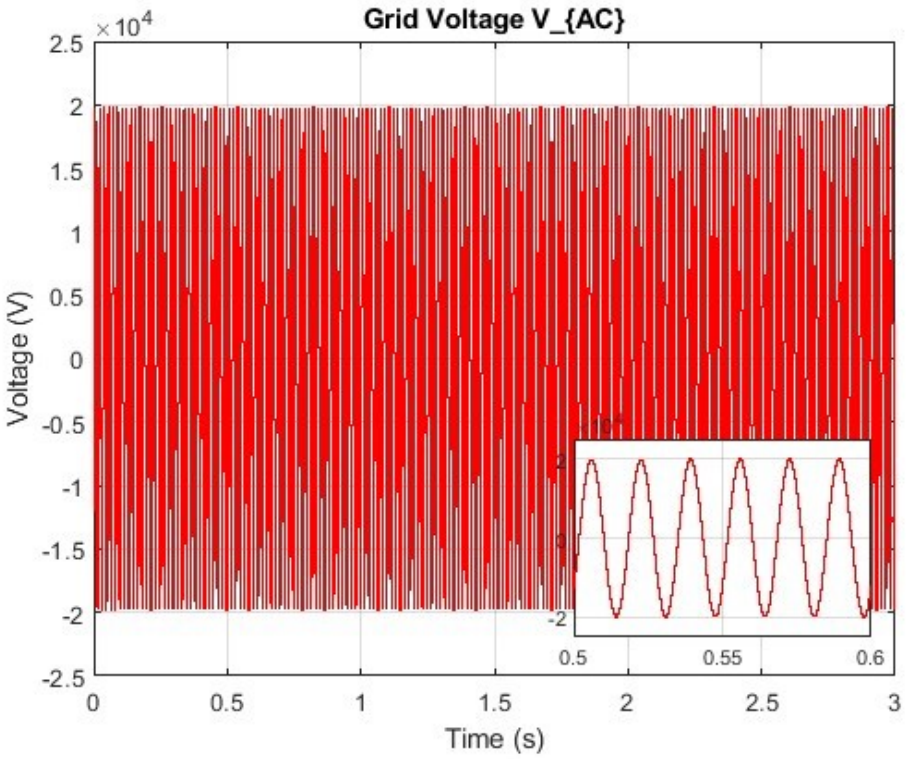

Figure 2.10: Vac under Standard Irradiation – Topology 1

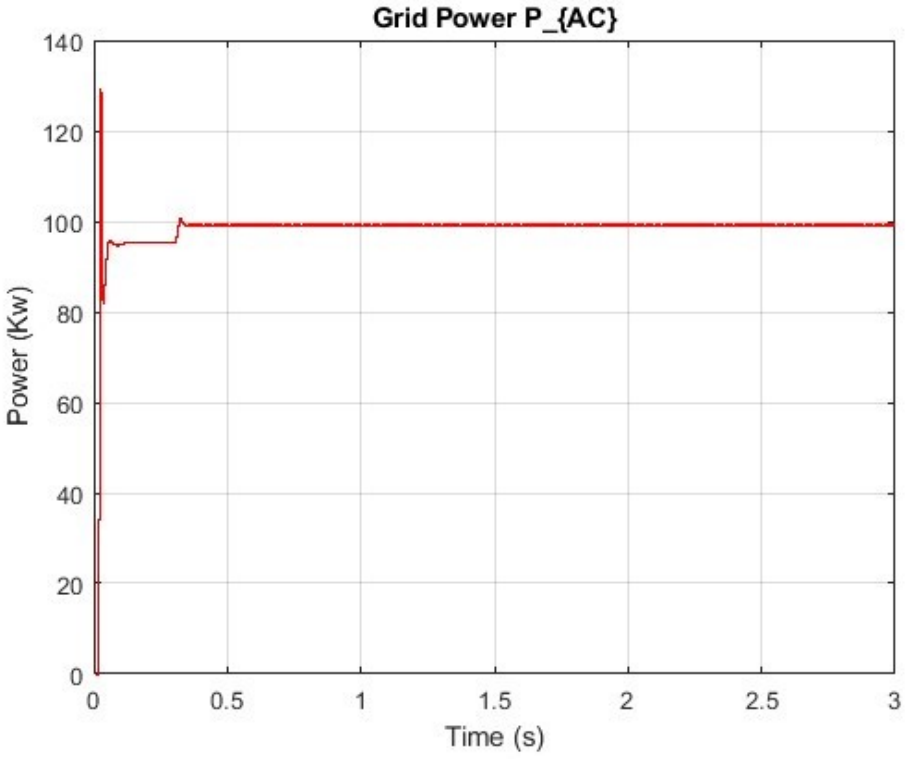

Figure 2.11: Pgrid under Standard Irradiation – Topology 1

Under partial shading:

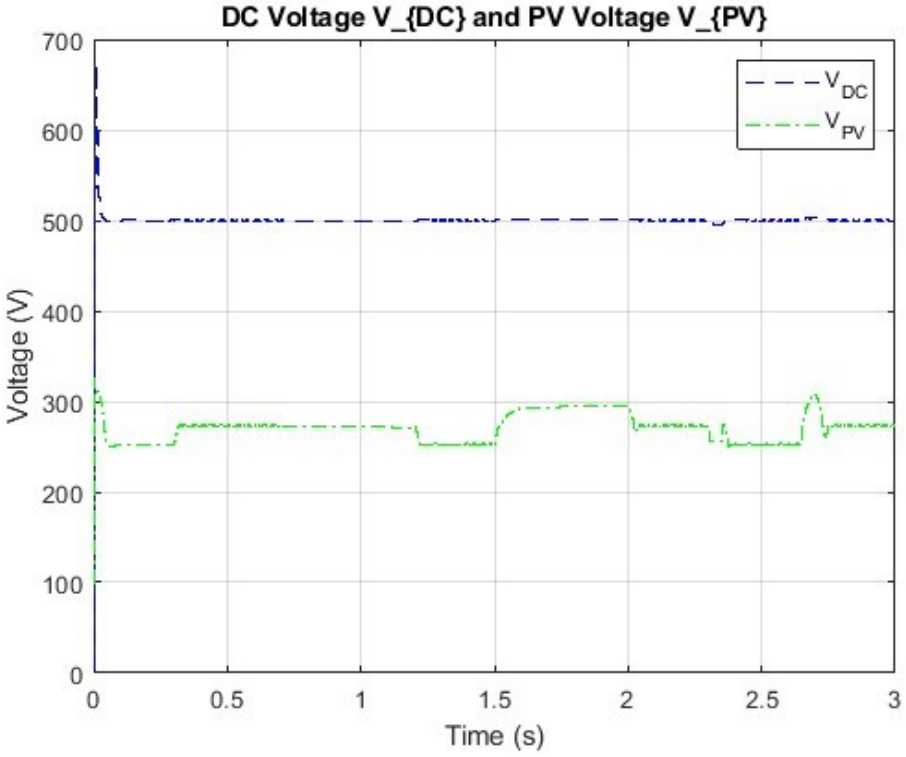

Figure 2.12: Vdc and Vpv under Partial Shading – Topology 1

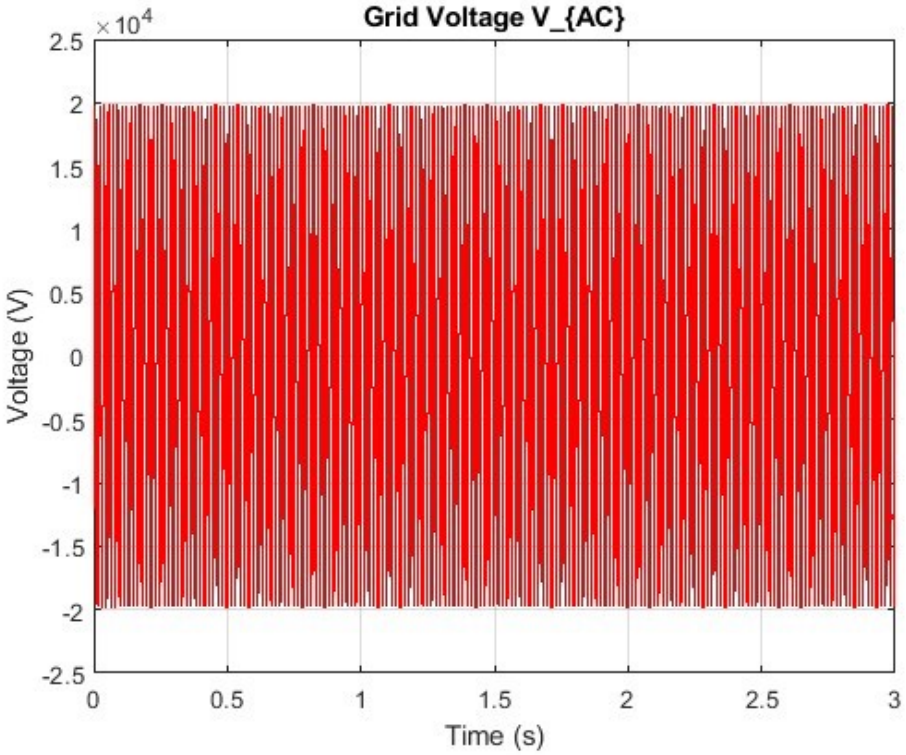

Figure 2.13: Vac under Partial Shading – Topology 1

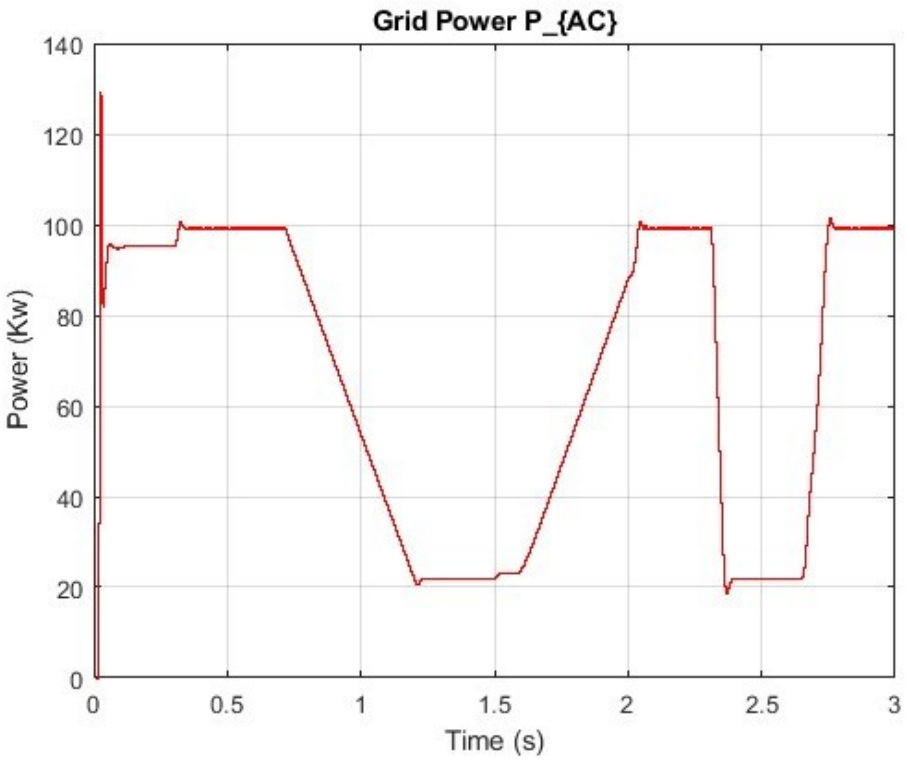

Figure 2.14: Pgrid under Partial Shading – Topology 1

Under standard irradiation, the system is stable with $V_{\text{dc}} = 500\,\text{V}$, $V_{\text{pv}} \approx 270\,\text{V}$, and $P_{\text{grid}} \approx 100\,\text{kW}$.

However, during partial shading, V_{dc} remains constant, but V_{pv} fluctuates (250–290 V), and P_{grid} drops sharply (down to 20 kW), following the irradiance variations directly. V_{ac} remains similar in both cases.

2.3.2 Topology 2: Two Series PVs + Single Boost Converter

Connecting two PV panels in series with one boost converter increases the overall voltage, which can improve boost converter efficiency. This setup also remains relatively simple and cost-effective.

Under standard irradiance (1000 W/m^2)**:**

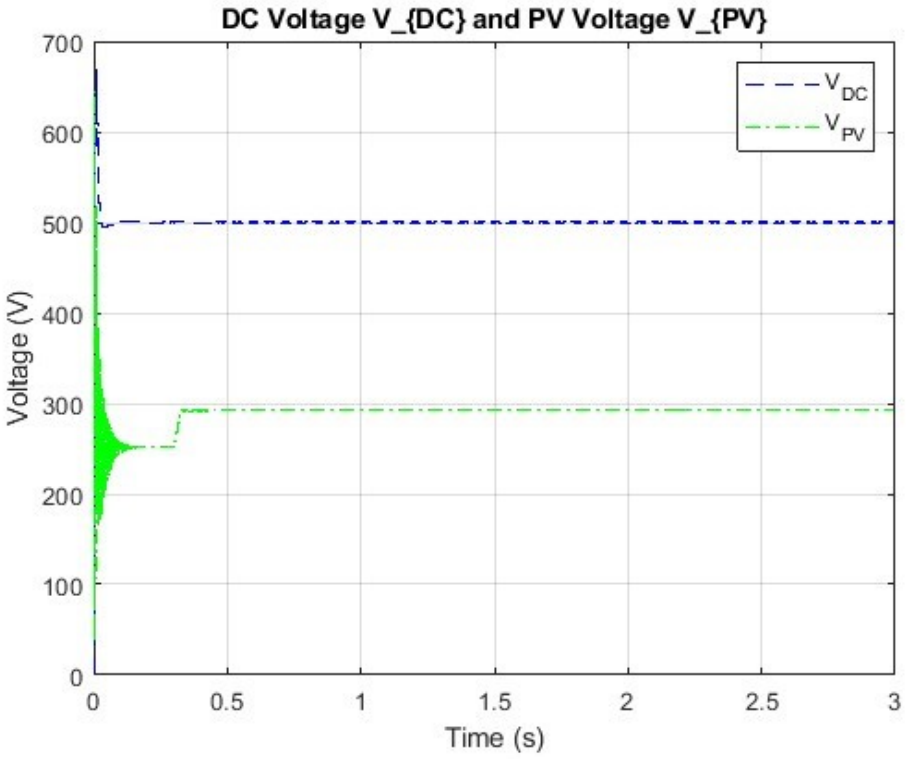

Figure 2.15: Vdc and Vpv under Standard Irradiation – Topology 2

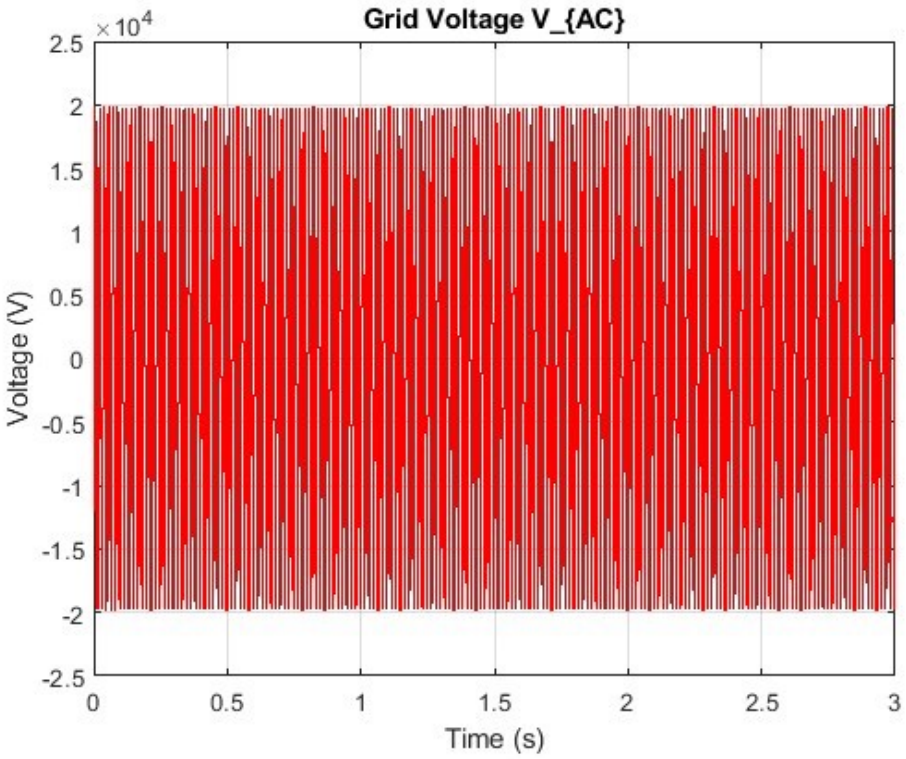

Figure 2.16: Vac under Standard Irradiation – Topology 2

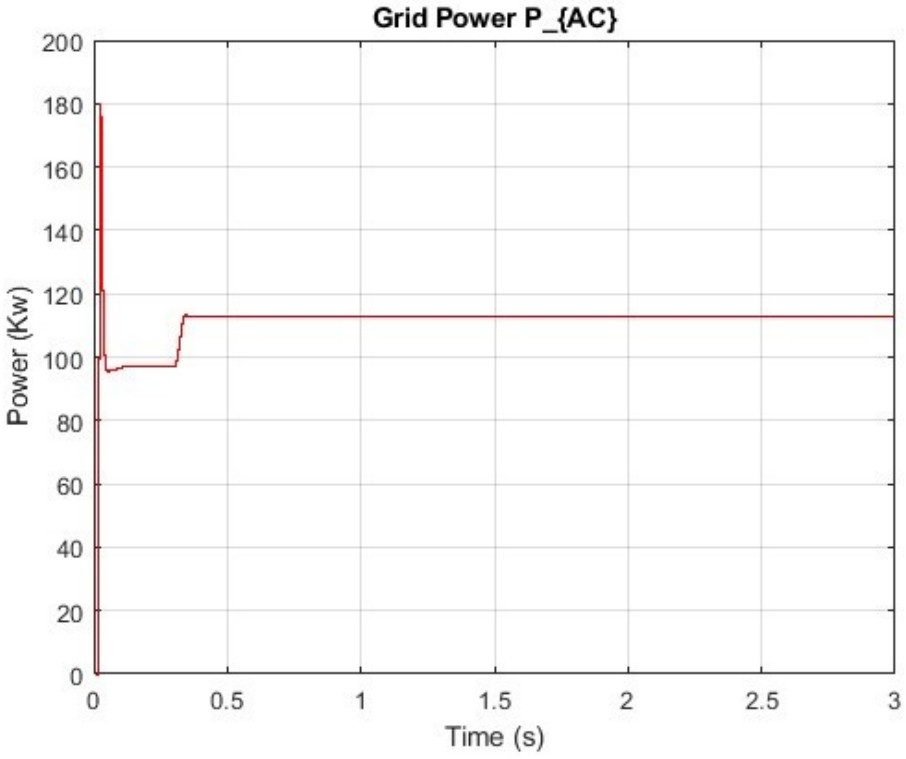

Figure 2.17: Pgrid under Standard Irradiation – Topology 2

Under partial shading:

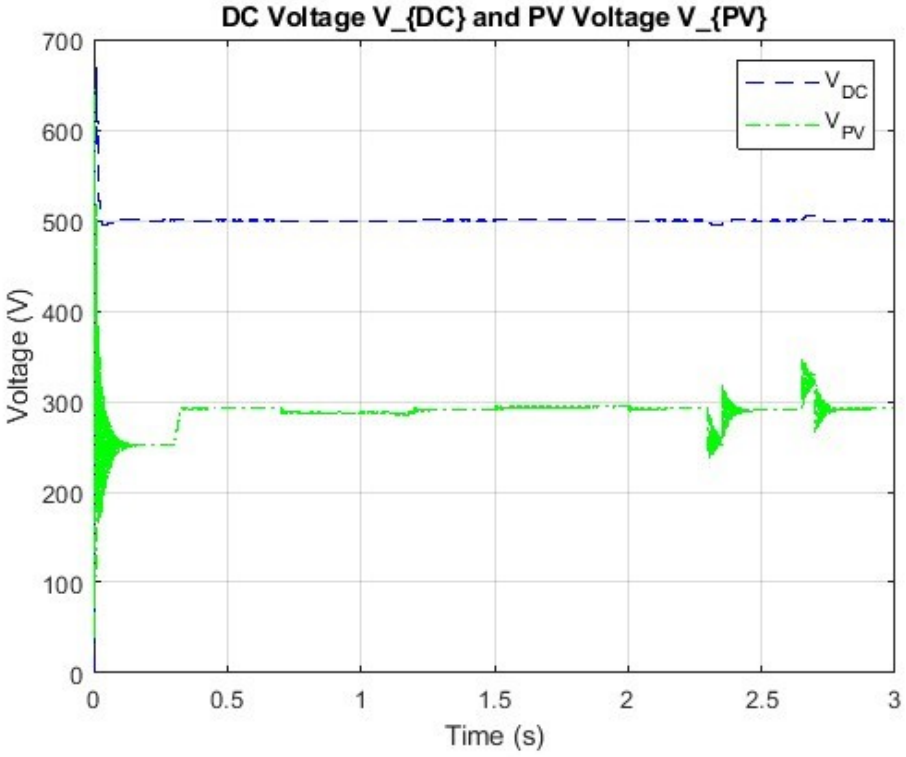

Figure 2.18: Vdc and Vpv under Partial Shading – Topology 2

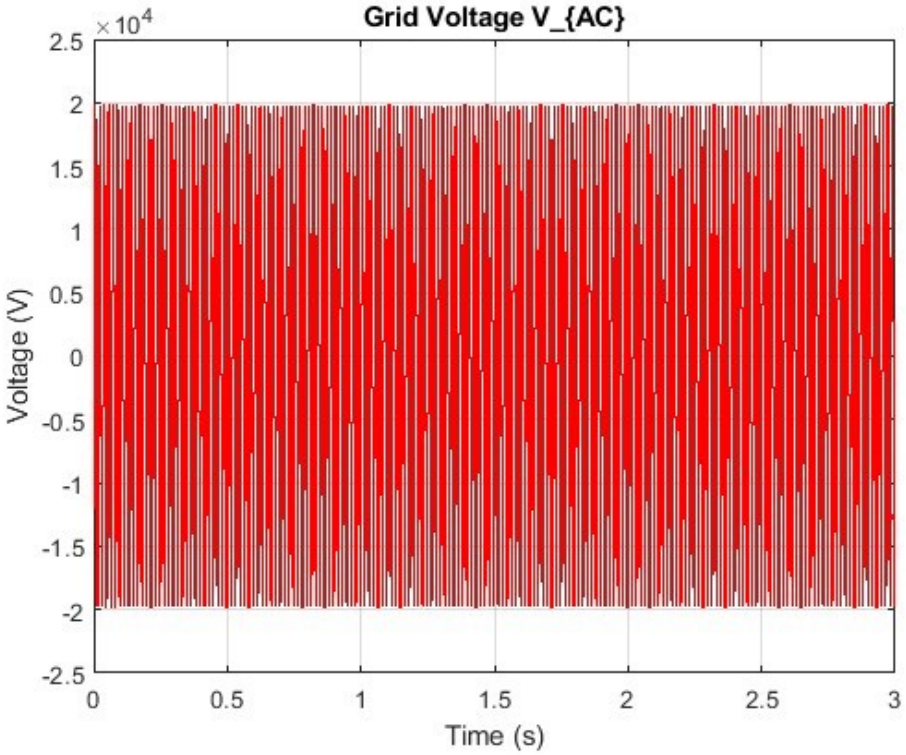

Figure 2.19: Vac under Partial Shading – Topology 2

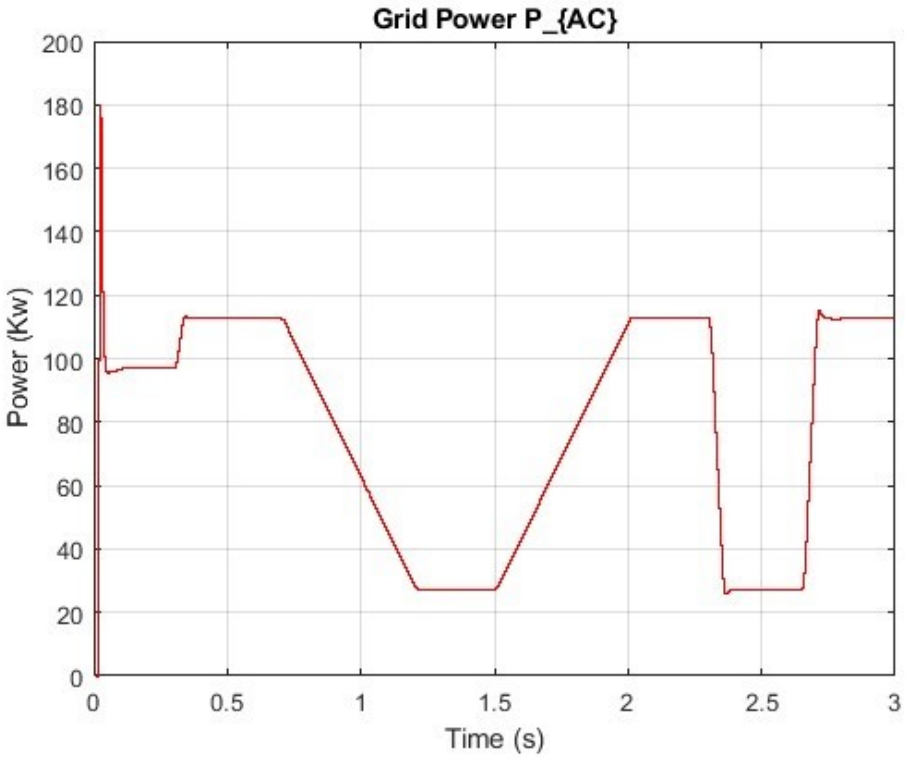

Figure 2.20: Pgrid under Partial Shading – Topology 2

Under standard irradiation conditions, the DC-link voltage (V_{dc}) quickly stabilizes at 500 V, while the PV voltage (V_{pv}) exhibits initial oscillations before settling around 300 V. The power delivered to the grid (P_{grid}) reaches approximately 117 kW. Under partial shading, V_{dc} remains at 500 V, but the system becomes unstable, particularly during abrupt changes in irradiance (I_r). The PV voltage (V_{pv}) becomes highly unstable, and P_{grid} drops to around 30 kW before gradually recovering as the irradiance improves.

2.3.3 Topology 3: Two Parallel PVs + Single Boost Converter

In this topology, two PV panels are connected in parallel to a single boost converter.

Under standard irradiance (1000 W/m^2)**:**

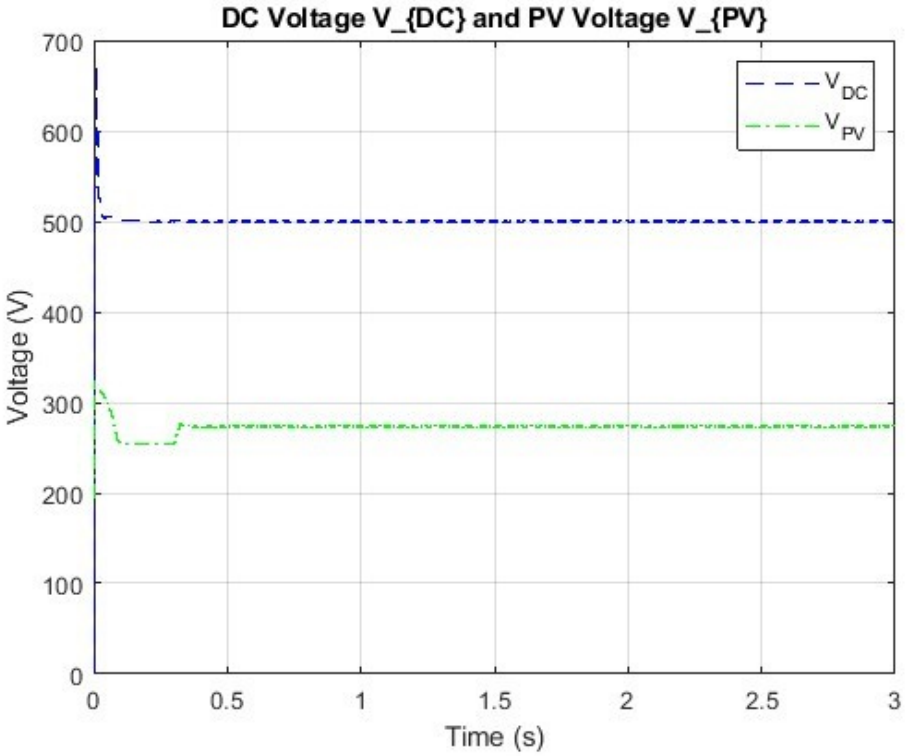

Figure 2.21: Vdc and Vpv under Standard Irradiation – Topology 3

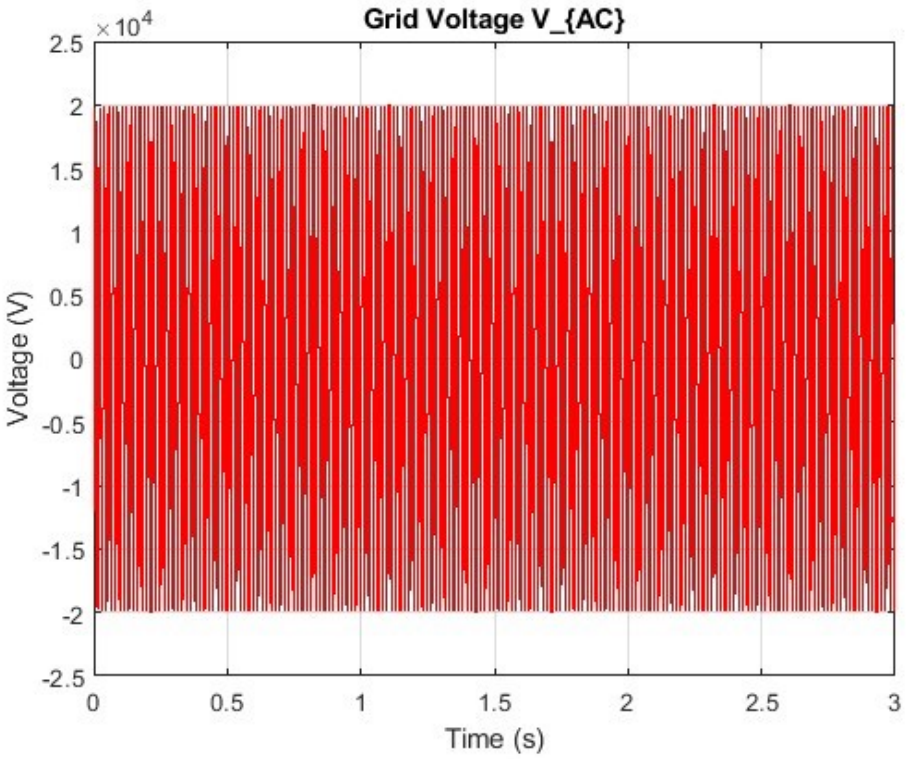

Figure 2.22: Vac under Standard Irradiation – Topology 3

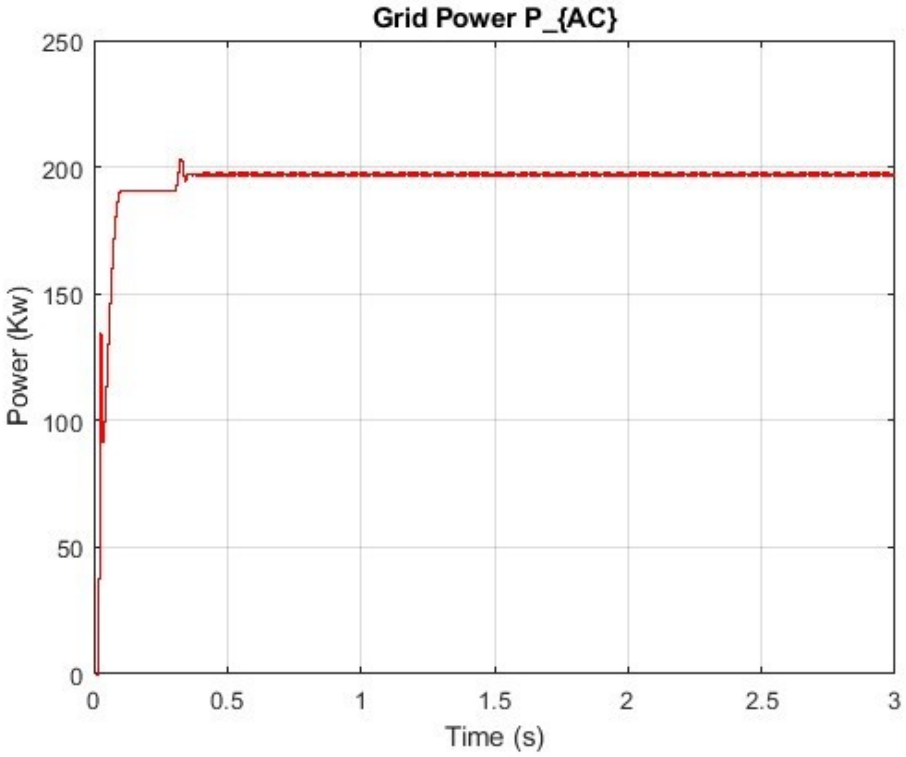

Figure 2.23: Pgrid under Standard Irradiation – Topology 3

Under partial shading:

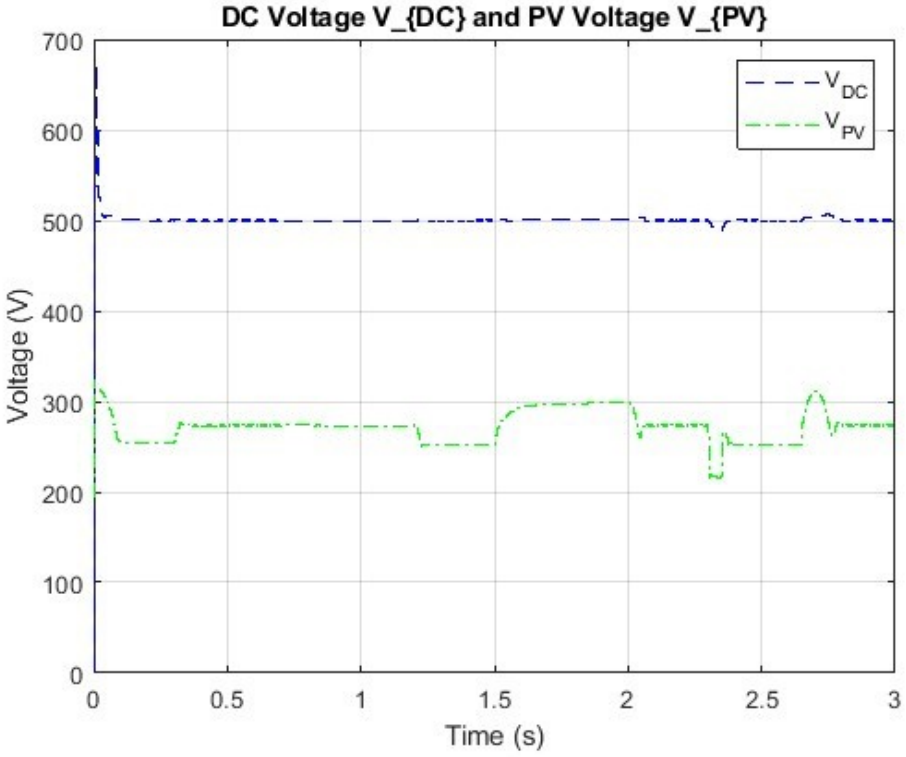

Figure 2.24: Vdc and Vpv under Partial Shading – Topology 3

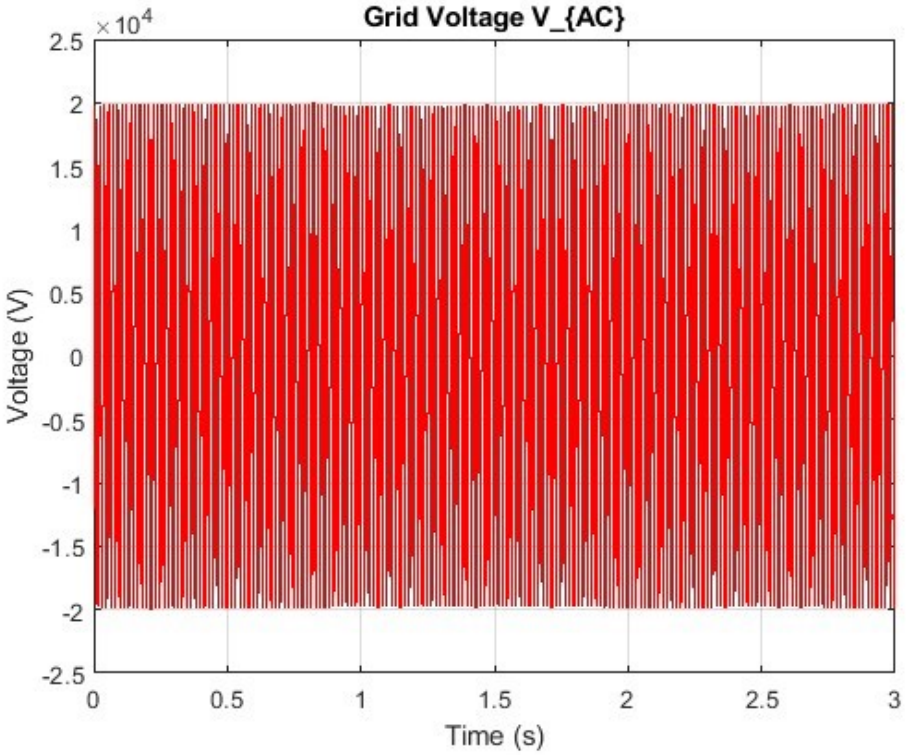

Figure 2.25: Vac under Partial Shading – Topology 3

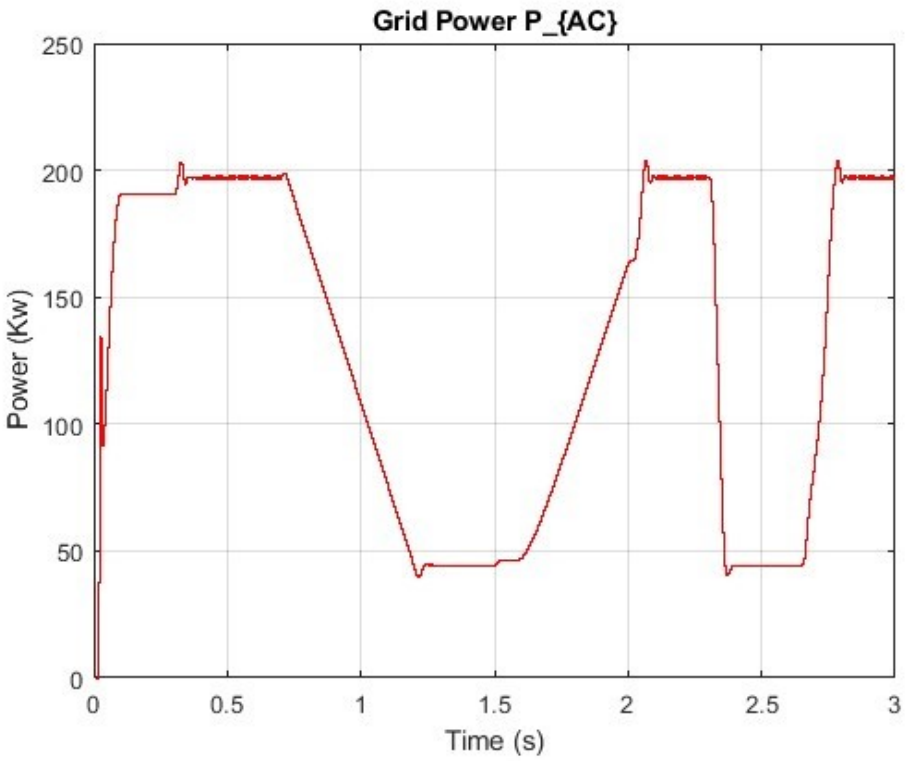

Figure 2.26: Pgrid under Partial Shading – Topology 3

Under standard irradiation, the system remains stable with $V_{\text{dc}} = 500$ V, $V_{\text{pv}} \approx 270$ V (smooth), and P_{grid} rising with initial oscillations before stabilizing around 190–198 kW. During partial shading, V_{dc} remains constant, but the system exhibits noticeable instability, especially during sudden irradiance variations. V_{pv} becomes unstable, and P_{grid} drops to around 45 kW, indicating better shading tolerance and gradual recovery as irradiance improves.

2.3.4 Topology 4: Two PVs with Separate Boost Converters (Series Output)

This topology assigns a dedicated boost converter to each PV panel, and the converters' outputs are connected in parallel. The key benefit here is the ability to apply independent MPPT algorithms to each panel.

Under standard irradiance (1000 W/m^2)**:**

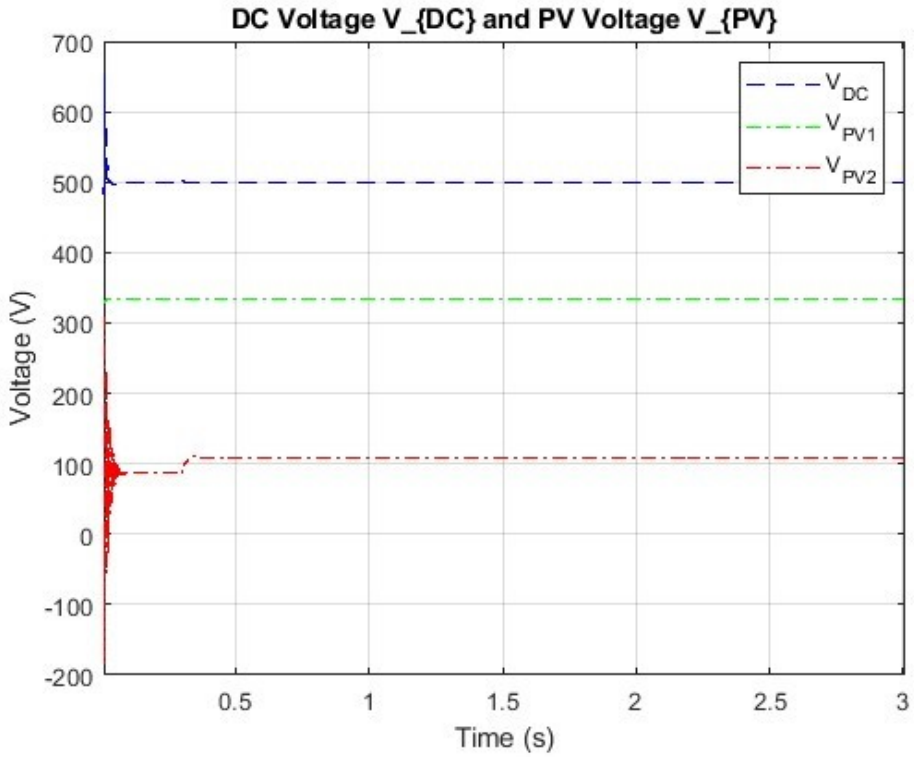

Figure 2.27: Vdc and Vpv under Standard Irradiation – Topology 4

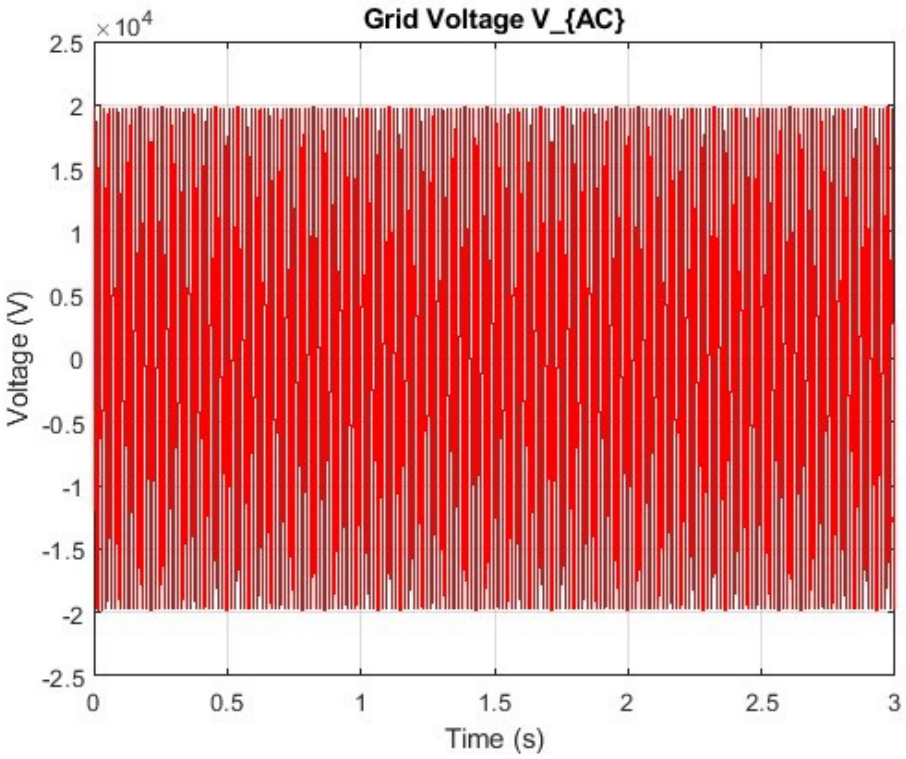

Figure 2.28: Vac under Standard Irradiation – Topology 4

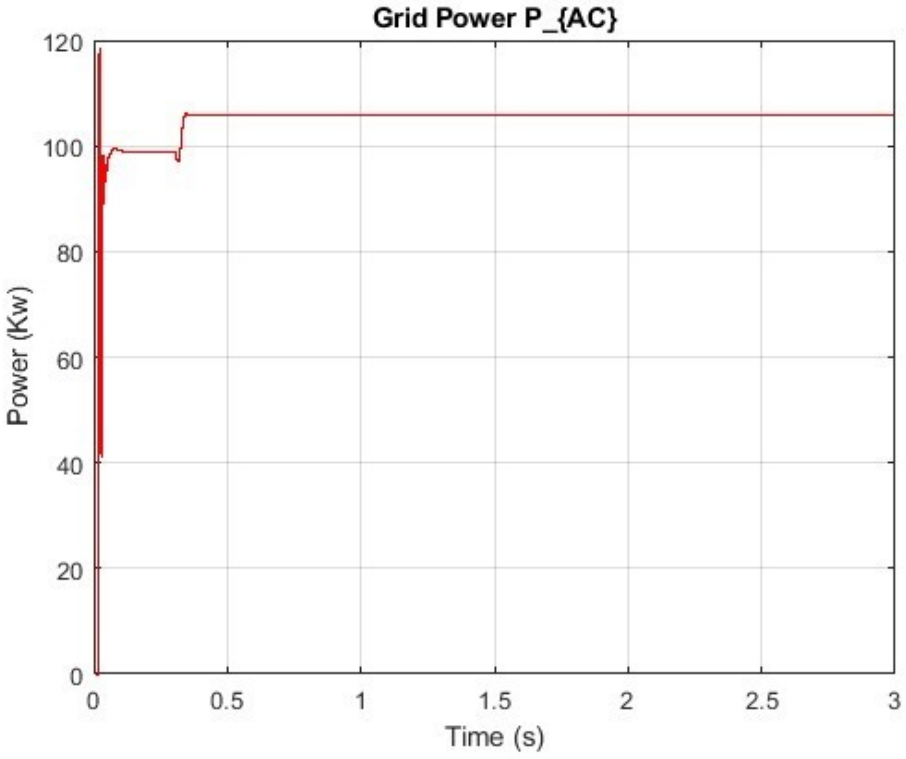

Figure 2.29: Pgrid under Standard Irradiation – Topology 4

Under partial shading:

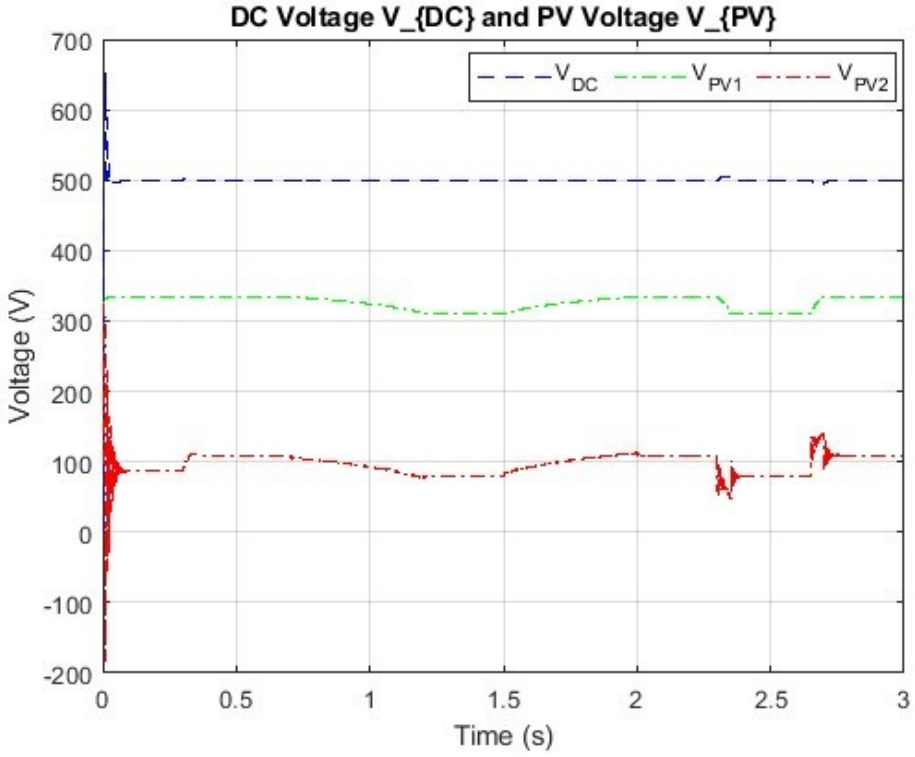

Figure 2.30: Vdc and Vpv under Partial Shading – Topology 4

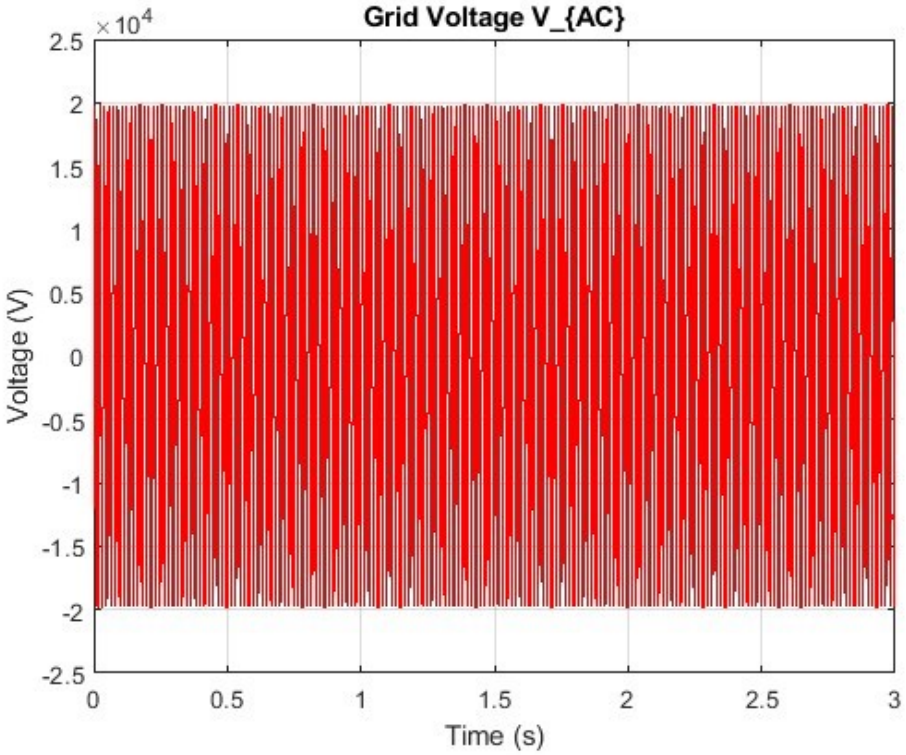

Figure 2.31: Vac under Partial Shading – Topology 4

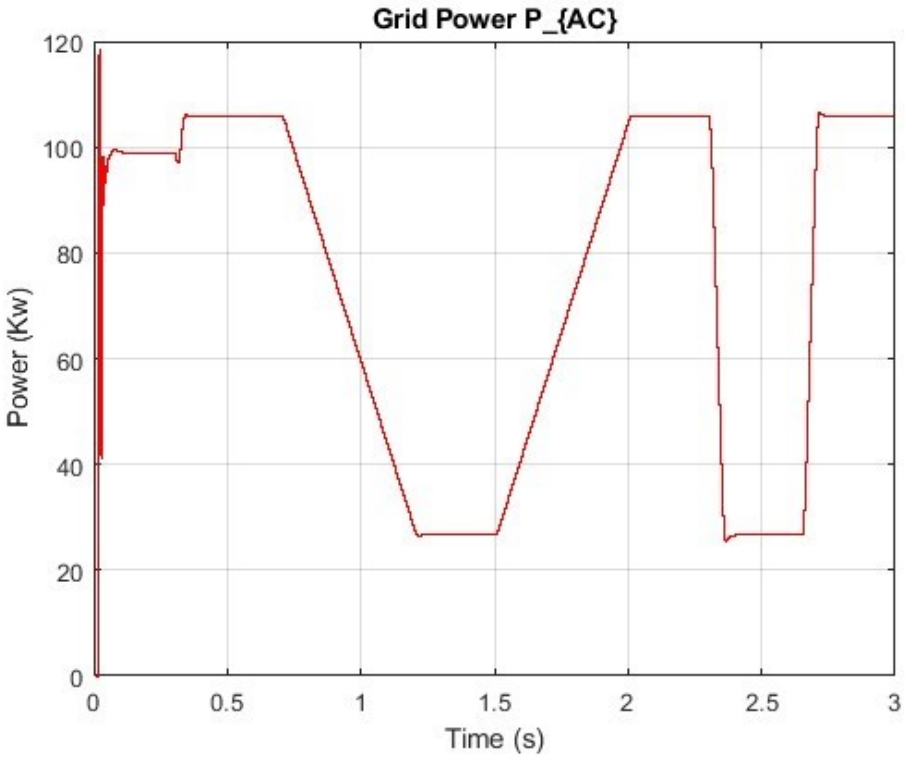

Figure 2.32: Pgrid under Partial Shading – Topology 4

Under standard irradiation, the system is stable with $V_{\text{dc}} = 500$ V (no oscillations). V_{pv1} remains optimal around 340 V, while V_{pv2} shows initial oscillations before settling near 100 V. P_{grid} reaches 100 kW, stabilizing after initial fluctuations.During partial shading, V_{dc} remains stable with only minor disturbances during sudden irradiance changes. V_{pv1} stays above 300 V with minimal oscillations, while V_{pv2} holds around 100 V with more noticeable ripples. P_{grid} follows the irradiance drop to about 30 kW, then recovers accordingly.

2.3.5 Topology 5: Two PVs with Separate Boost Converters (Parallel Output)

Similar to the previous topology, each PV panel has its own boost converter with independent MPPT. However, the converters outputs are connected in series.

Under standard irradiance (1000 W/m^2)**:**

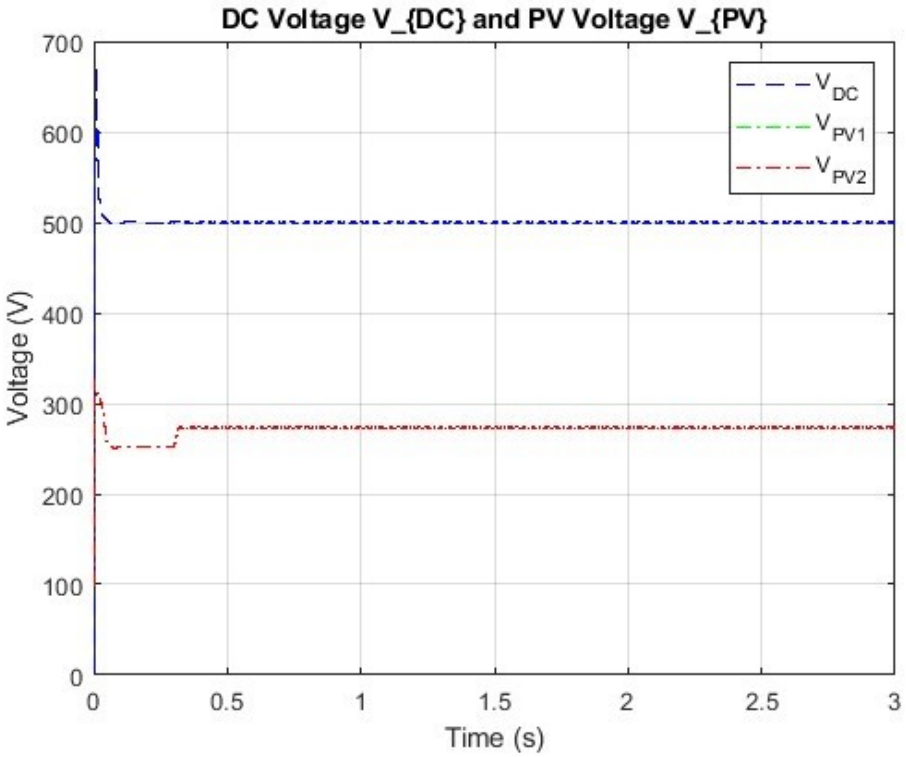

Figure 2.33: Vdc and Vpv under Standard Irradiation – Topology 5

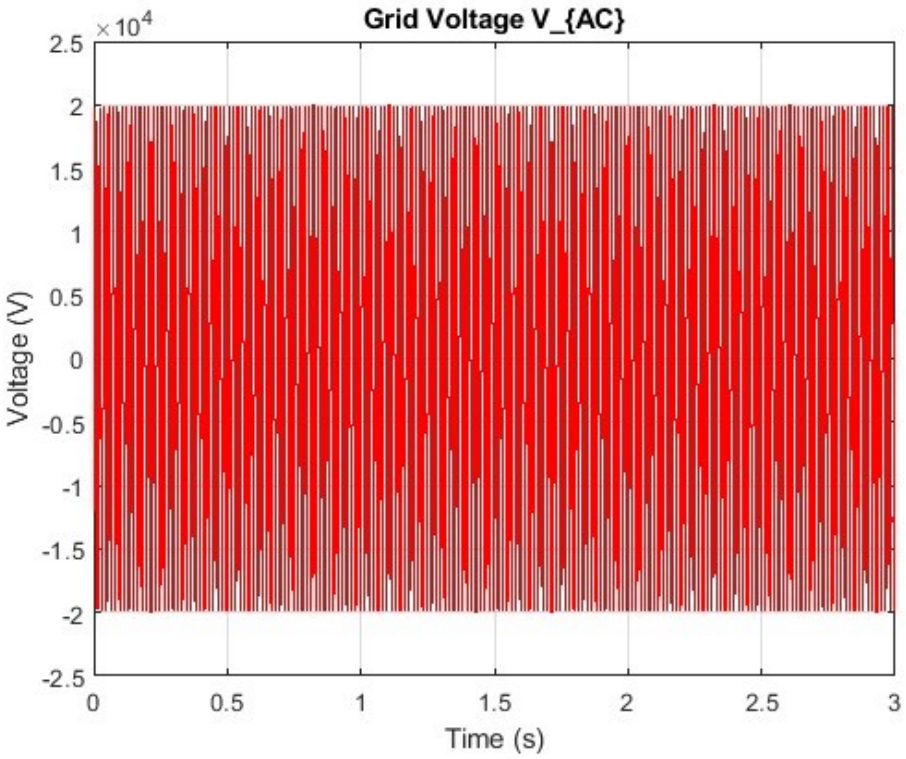

Figure 2.34: Vac under Standard Irradiation – Topology 5

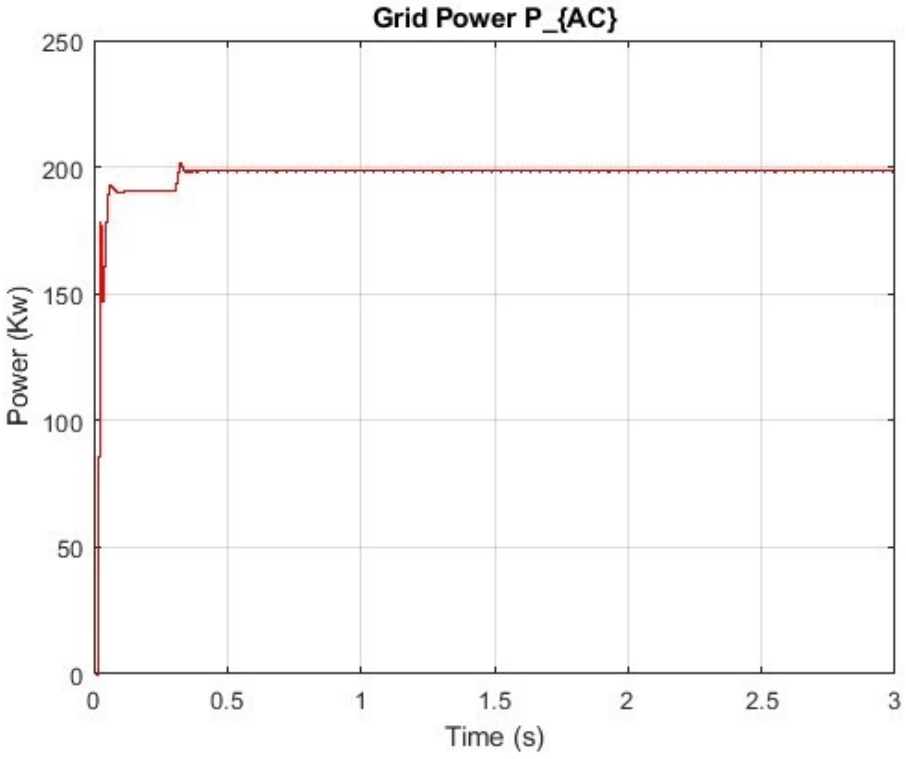

Figure 2.35: Pgrid under Standard Irradiation – Topology 5

Under partial shading:

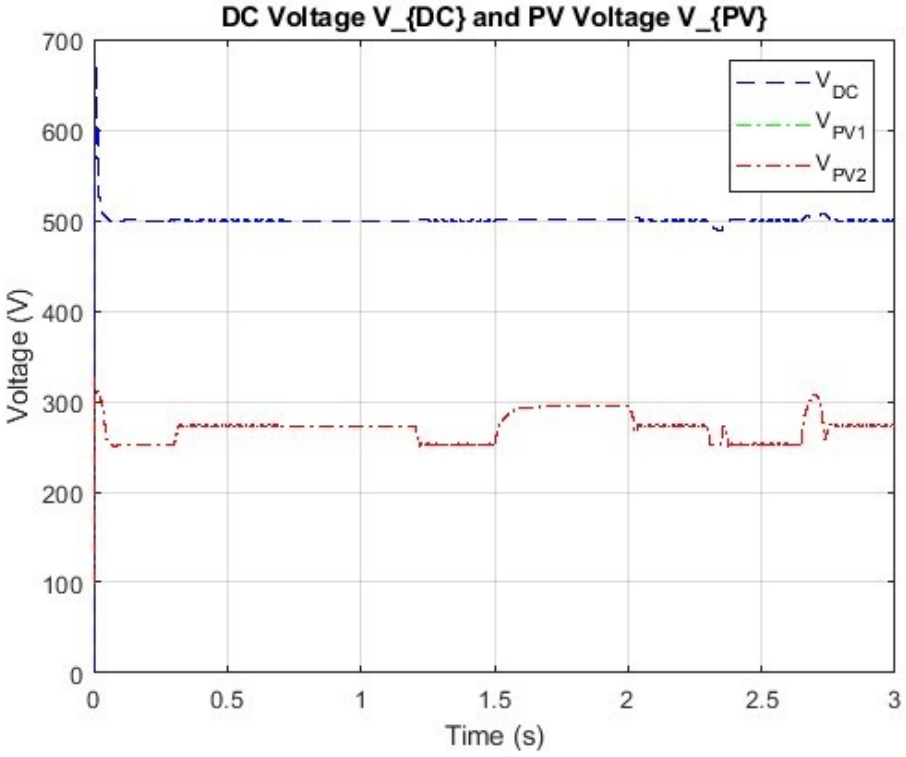

Figure 2.36: Vdc and Vpv under Partial Shading – Topology 5

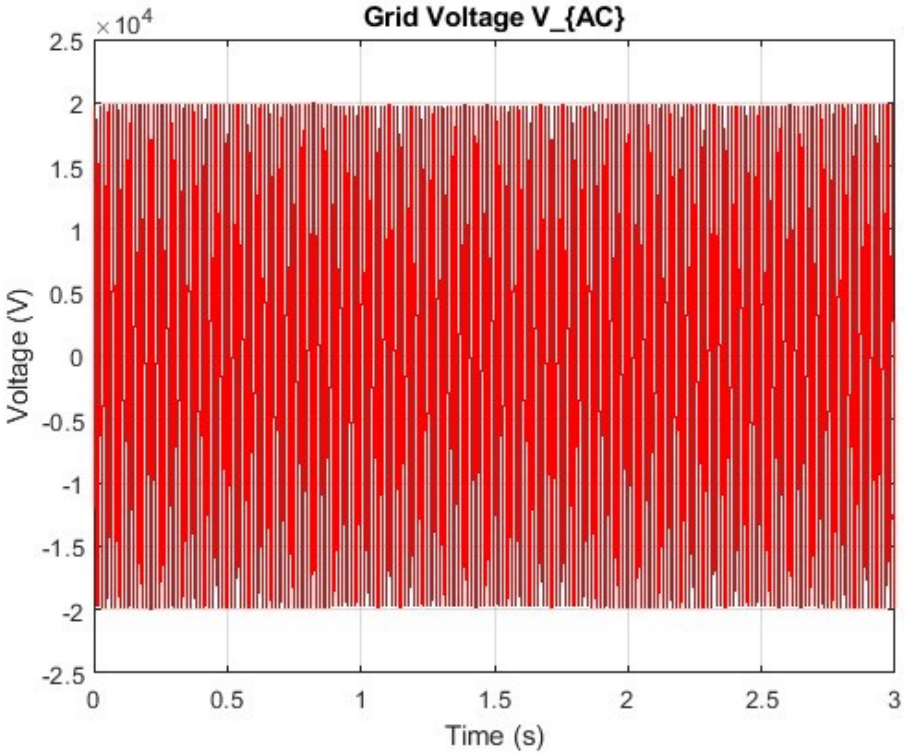

Figure 2.37: Vac under Partial Shading – Topology 5

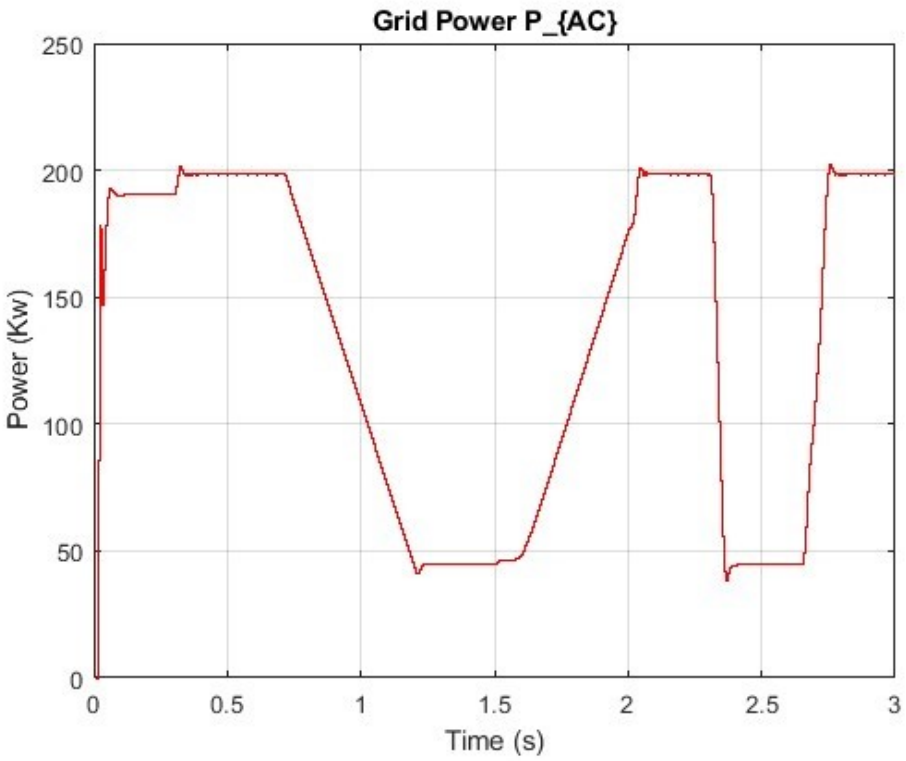

Figure 2.38: Pgrid under Partial Shading – Topology 5

Under standard irradiation, Topology 5 maintains a constant DC voltage of 500 V with stable and equal PV voltages ($V_{\text{pv1}} = V_{\text{pv2}}$) around 270 V, resulting in a steady grid power output near 200 kW. During partial shading with fluctuating irradiance, the DC voltage remains stable, but both PV voltages become unstable, following rapid changes in irradiance. Grid power correspondingly drops to about 50 kW during shading and recovers as irradiance increases.

2.4 Comparative Analysis

This section presents a comparative analysis of five different PV system topologies interfaced with boost converters, under two operating conditions: **standard irradiance** and **partial shading**. The evaluation is based on key performance indicators, primarily:

- DC-link voltage stability (V_{dc})
- Grid-injected power (P_{grid})
- Dynamic response under shading
- MPPT effectiveness
- System complexity and cost

First, we compare the V_{dc} voltage results of all five topologies by plotting them in the same figure, under two conditions: standard irradiance (1000 W/m^2) in Fig. 2.39, and partial shading in Fig. 2.40.

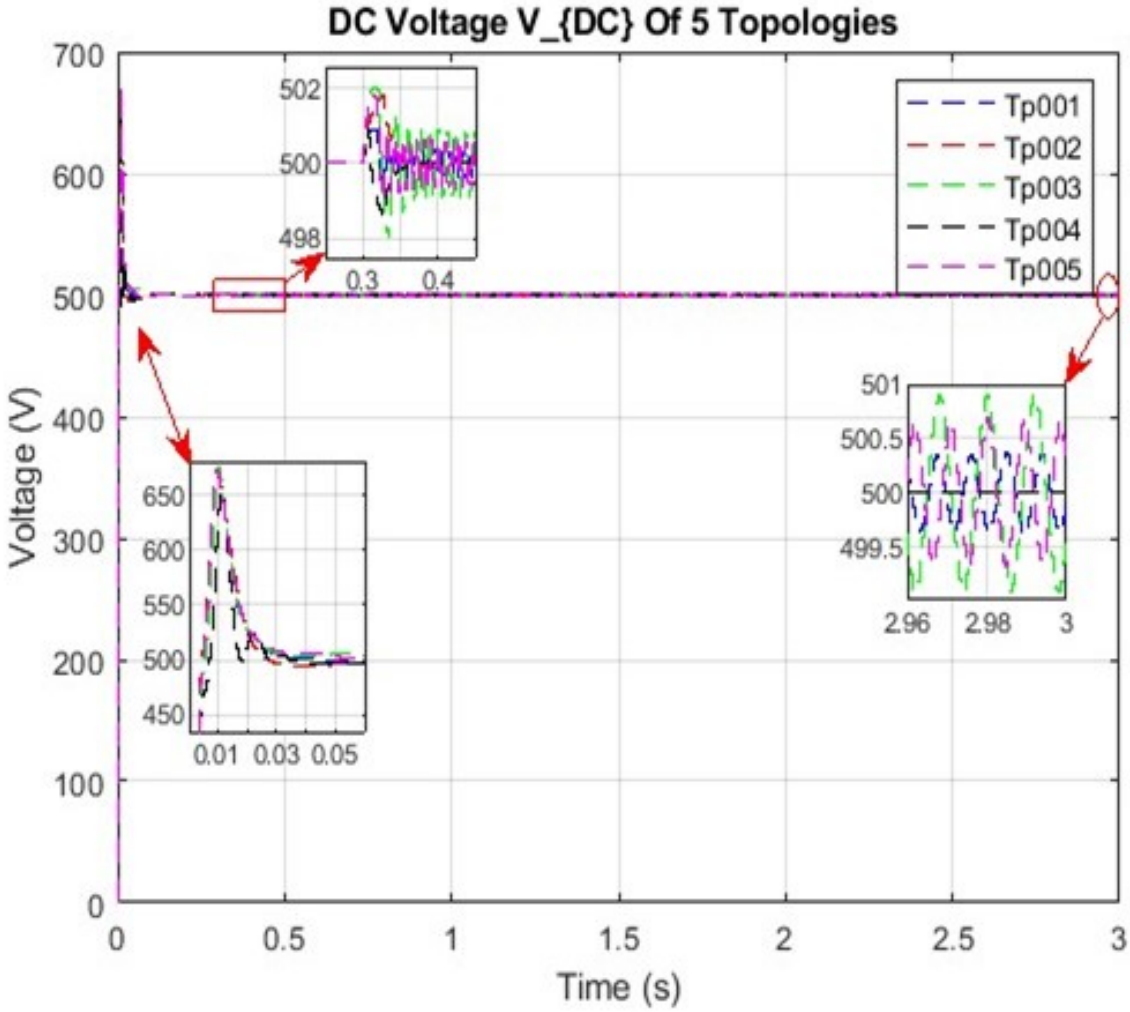

Figure 2.39: Comparison of V_{dc} across all topologies under standard irradiance (1000 W/m^2)

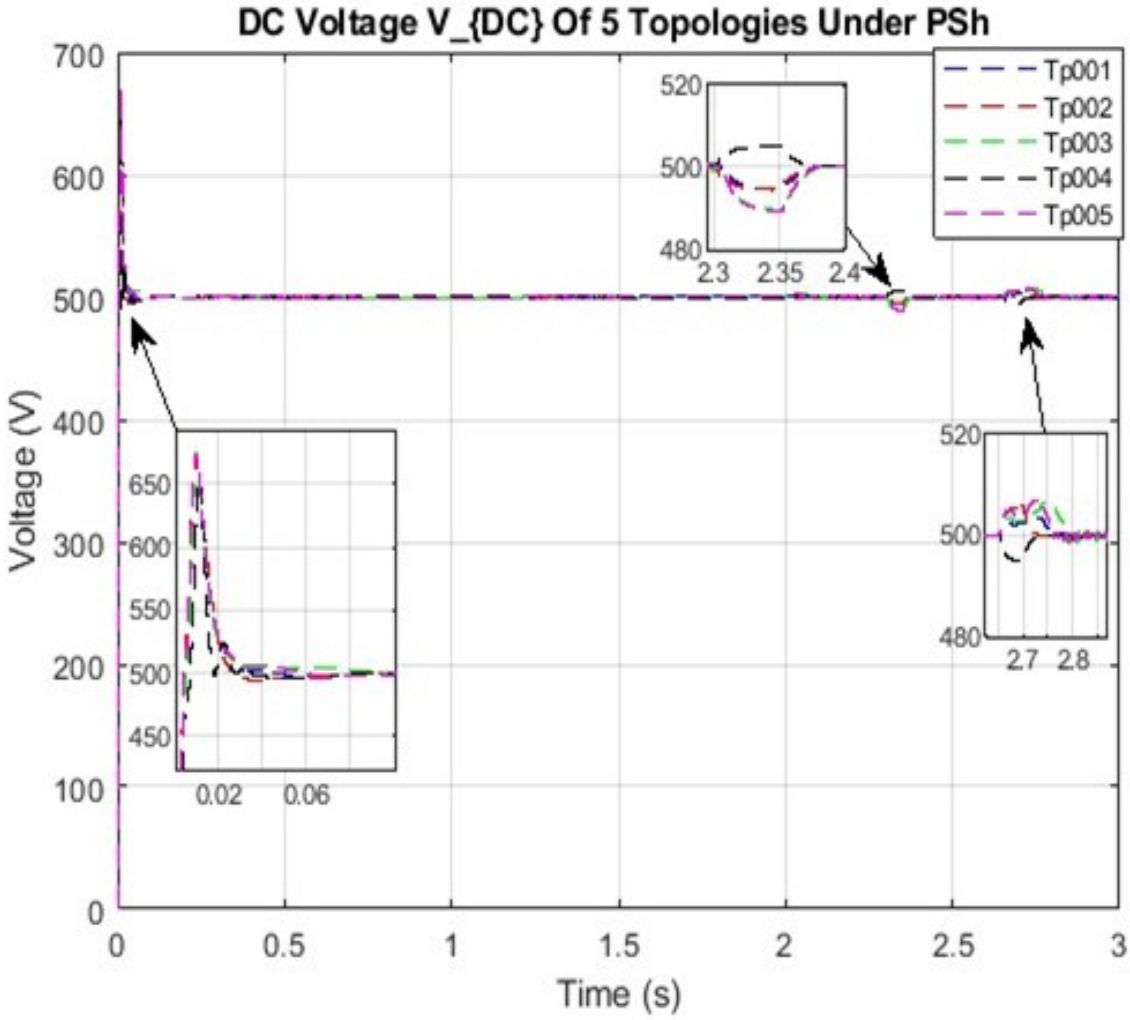

Figure 2.40: Comparison of V_{dc} across all topologies under partial shading condition

In both cases, the V_{dc} voltage remains approximately constant at 500 V, with differences in stability levels and speed of recovery.Under standard irradiation, TP002 and TP004 topologies show excellent stability, while TP001 experiences small variations, and TP003 and TP005 are the least stable.Under partial shading, the topologies continue to maintain good stability with minor disturbances during sudden irradiance changes. However, TP002 and TP004 demonstrate faster recovery, while TP003 and TP005 are more sensitive and affected by rapid irradiance variations.

After that, we compare the P_{grid} power results of all five topologies by plotting them in the same figure under two conditions: standard irradiance (1000 W/m^2) in Fig. 2.41, and partial shading in Fig. 2.42.

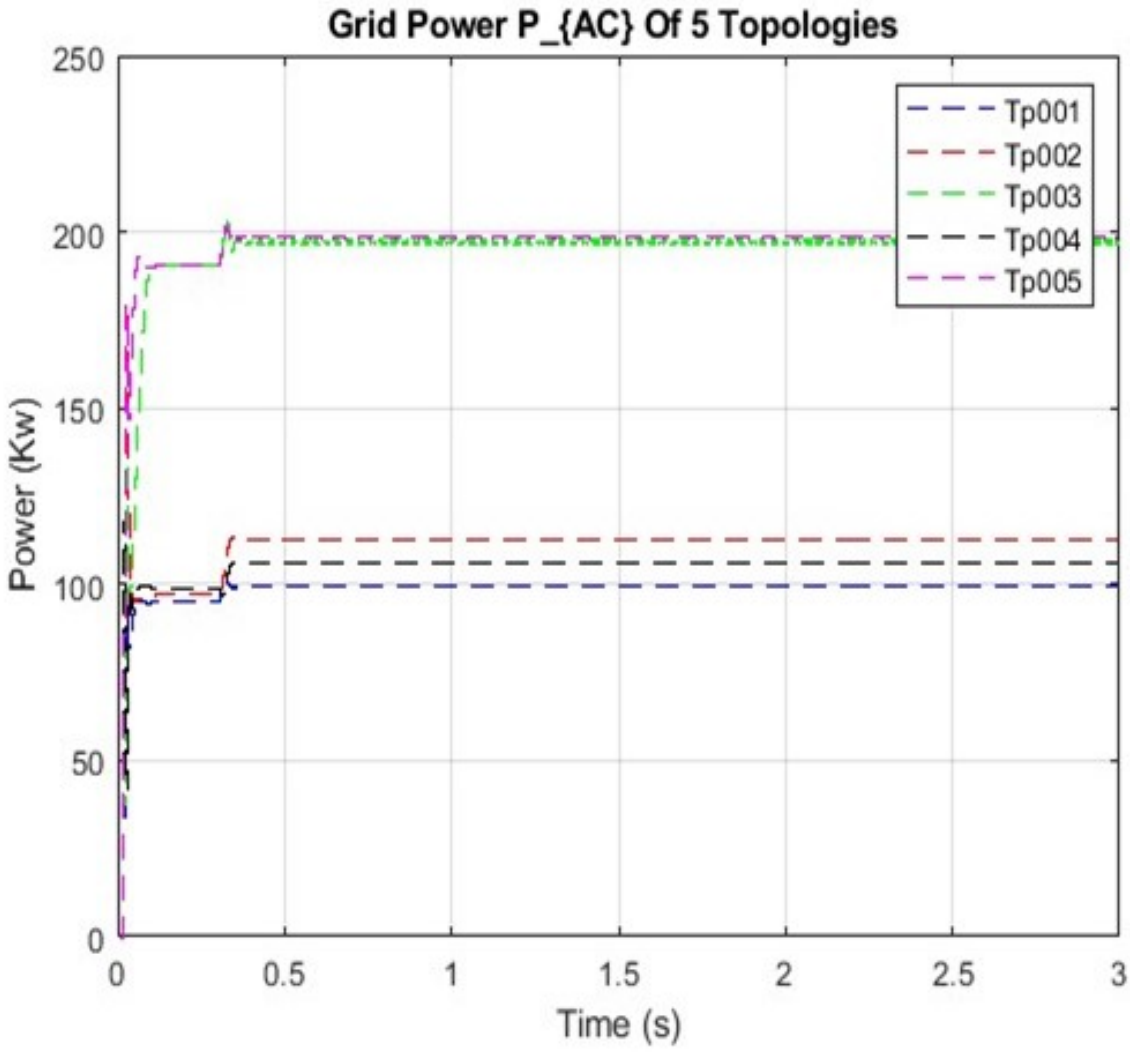

Figure 2.41: Comparison of P_{grid} across all topologies under standard irradiance (1000 W/m^2)

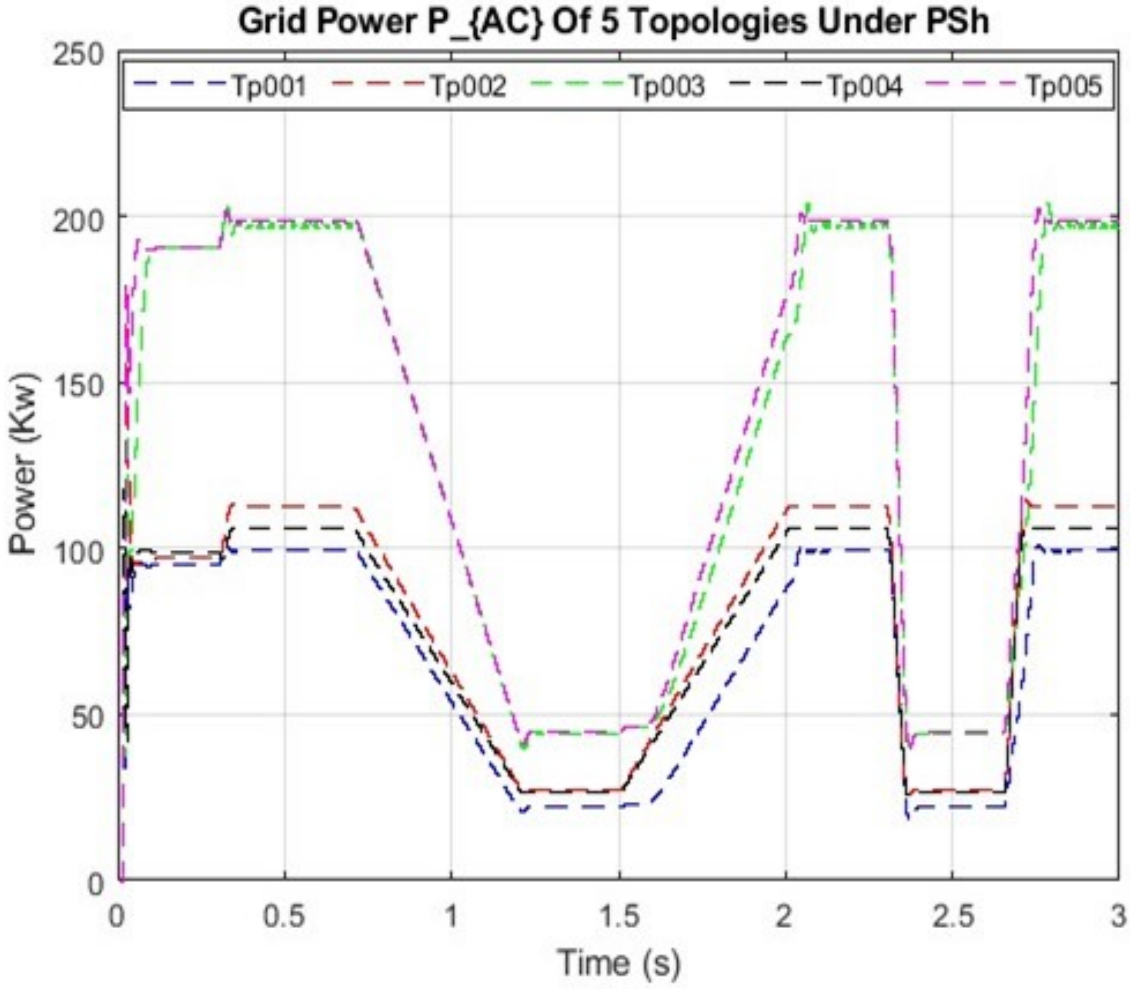

Figure 2.42: Comparison of P_{grid} across all topologies under partial shading condition

The analysis of P_{grid} across the five converter topologies under both standard and partial shading conditions reveals notable differences in power performance.

Under standard irradiation, TP005 consistently achieved the highest and most stable output (approximately 200 kW), followed by TP003 (190–198 kW), while TP001, TP002, and TP004 delivered lower outputs (approximately 100–117 kW).

In partial shading scenarios, TP005 again demonstrated superior resilience, maintaining a minimum power around 50 kW with smooth recovery. TP003 followed with better shading tolerance (around 45 kW minimum), whereas TP001, TP002, and TP004 showed deeper drops (down to 20–30 kW).

Overall, TP005 stands out as the most robust and efficient topology in both ideal and shaded conditions, making it the most favourable choice in environments prone to irradiance variation.

We observe the effect of connection type (series vs. parallel): topologies with parallel configurations (TP003 and TP005) showed better performance and shading tolerance. This is because each PV module can operate independently at its own maximum power point without being forced to match the others.

In contrast, series configurations (TP002 and TP004) suffer from mismatch issues—since the current must be equal, a shaded module can limit the performance of the entire string.

Additionally, TP004 employs separate converters connected in series at the output. While this offers modularity, the need for current matching and the lack of MPPT coordination lead to voltage imbalances between V_{pv1} and V_{pv2}.

In conclusion, considering both the response to partial shading and system cost, TP005 offers the best electrical performance and robustness under shading. However, it is also the most expensive due to the use of two converters and a fully parallel architecture.

On the other hand, TP001 and TP002 are more economical and simpler to implement but suffer from performance limitations under partial shading. TP003 strikes a balance between performance and cost, making it suitable for mid-level budgets.

2.5 Conclusion

In this chapter, we presented a comprehensive analysis of five different boost converter topologies for photovoltaic (PV) systems under both standard and partial shading conditions. We began by introducing the PV system, detailing its main components: the PV array, boost converter, MPPT algorithm, and voltage source converter.

During the simulation phase, we used MATLAB/Simulink to evaluate each topology's dynamic behaviour. Key parameters such as DC link voltage (V_{dc}), PV array voltage (V_{pv}), and grid power (P_{grid}) were monitored and compared under varying irradiance levels. The results revealed how each configuration responds to changes in sunlight, with particular emphasis on voltage stability and power delivery performance.

General Conclusion

In this dissertation, a detailed comparative study of five photovoltaic (PV) system topologies integrated with boost converter configurations was presented. The primary objective was to evaluate the performance of these topologies under both standard irradiance and partial shading conditions, with a focus on power conversion efficiency, MPPT accuracy, voltage stability, and resilience to environmental disturbances.

The simulation results, conducted in MATLAB/Simulink, demonstrated that topology-specific characteristics significantly influence the overall system behavior. While simpler topologies such as TP001 (single PV with single boost converter) and TP002 (two series PVs with single converter) offer ease of implementation and reduced cost, they suffer from pronounced efficiency losses under partial shading. In contrast, advanced architectures such as TP005, which employs separate converters for each PV unit with parallel output, consistently outperformed others in both irradiance scenarios. This topology enabled independent MPPT per module, resulting in enhanced shading tolerance and maximum power extraction.

The findings confirm that optimizing PV system design requires careful consideration of converter topology, particularly in environments prone to shading or mismatch. The work contributes to the body of knowledge in PV integration by providing quantitative benchmarks and design trade-offs, offering valuable guidance for researchers, engineers, and system planners. Future work may explore hybrid MPPT methods, hardware implementation, and the application of artificial intelligence for real-time adaptation.

Ultimately, this dissertation underscores the vital role of power electronics in the sustainable deployment of solar energy systems, reinforcing the vision of a cleaner and more reliable energy future.

Bibliography

[1] T. Esram and P. L. Chapman, "Comparison of photovoltaic array maximum power point tracking techniques," *IEEE Transactions on Energy Conversion*, vol. 22, no. 2, pp. 439–449, 2007.

[2] N. Kapri, "Performance analysis and comparative study of different types of dc-dc converters," *International Research Journal on Advanced Science Hub*, vol. 1, no. 2, December 2019.

[3] H. Patel and V. Agarwal, "Matlab-based modeling to study the effects of partial shading on pv array characteristics," *IEEE Transactions on Energy Conversion*, vol. 23, no. 1, pp. 302–310, 2008.

[4] J. A. Duffie and W. A. Beckman, *Solar Engineering of Thermal Processes*, 4th ed. Wiley, 2013.

[5] M. A. Green, *Solar Cells: Operating Principles, Technology, and System Applications*. Prentice Hall, 1982.

[6] D. Sera, R. Teodorescu, and P. Rodriguez, "Pv panel model based on datasheet values," in *IEEE International Symposium on Industrial Electronics*, 2007, pp. 2392–2396.

[7] T. A. B. Raj and R. Ramesh, "Modelling and analysis of parallel boost converter for photovoltaic applications," *Journal of Theoretical and Applied Information Technology*, 2014.

[8] S. L. Shettigar and D. S. Kanchan, "Double boost converter for photovoltaic power-generation systems," *International Journal of Electrical & Electronic Engineering & Telecommunications*, 2015.

[9] F. Talha, K. Benmouiza, and M. Birane, "In-depth comparison of pv array configurations and boost converter topologies using p&o and pso techniques," *International Information and Engineering Technology Association (IIETA)*, 2024.

[10] D. K. Narne, T. A. R. Kumar, and R. K. R. Alla, "Evaluation of series-parallel-cross-tied pv array configuration performance with mppt techniques under partial shading conditions," *Clean Energy*, 2023.

[11] S. Seba, M. Birane, and K. Benmouiza, "A comparative analysis of boost converter topologies for photovoltaic systems using mppt (p&o) and beta methods under partial shading," *Revue Roumaine des Sciences Techniques, Série Électrotechnique et Énergétique*, 2023.

[12] M. H. Rashid, *Power Electronics: Circuits, Devices, and Applications*, 4th ed. Pearson, 2013.

[13] S. M. Belhadj, B. Meliani, H. Benbouhenni, I. Colak, Z. M. S. Elbarbary, and S. F. Al-Gahtani, "Control of three-level quadratic dc-dc boost converters for energy systems using various technique-based mppt methods," *Scientific Reports*, 2025.

[14] N. Karami, N. Moubayed, and R. Outbib, "General review and classification of different mppt techniques," *Renewable and Sustainable Energy Reviews*, 2017.

[15] E. W. Mukti, A. Risdiyanto, A. A. Kristi, and R. Darussalam, "Particle swarm optimization (pso)-based photovoltaic mppt algorithm under partial shading condition," *Journal of Electronics and Telecommunications*, 2023.

[16] Z. Fan, S. Li, H. Cheng, and L. Liu, "Perturb and observe mppt algorithm of photovoltaic system: A review," in *2021 Chinese Control and Decision Conference (CCDC)*. IEEE, 2021.

[17] N. K. Meena, A. Jaiswal, and H. K. Maheshwari, "A grid connected pv module having mppt and vsc," *International Journal for Science and Advance Research in Technology (IJSART)*, 2018.

[18] I. S. Subtil, "Modelling and control of vsc with a photovoltaic source," *The Polytechnic University of Catalonia*, 2021.